

APPLICATION OF LEARNING TECHNIQUES
TO AN INERTIAL NAVIGATION SYSTEM

By

WILLIAM ROBERT BARCLAY

Bachelor of Science in Electrical Engineering
Oklahoma State University
Stillwater, Oklahoma
1960

Master of Science in Electrical Engineering
Wichita State University
Wichita, Kansas
1963

Submitted to the faculty of the Graduate College of
the Oklahoma State University
in partial fulfillment of the requirements
for the degree of
DOCTOR OF PHILOSOPHY
May, 1968

OKLAHOMA
STATE UNIVERSITY
LIBRARY

OCT 24 1968

APPLICATION OF LEARNING TECHNIQUES
TO AN INERTIAL NAVIGATION SYSTEM

Thesis Approved:

Arthur M. Breipohl

Thesis Adviser

Kenneth A. McCollom

Paul G. McCollom

Jeanne Agnew

N. Durham

Dean of the Graduate College

688195

ACKNOWLEDGMENTS

I wish to express my sincere thanks to my thesis adviser, Professor A. M. Breipohl, for his help and guidance during my research. He has patiently devoted long hours on my behalf.

I am also indebted to two of my committee members, Professors Jeanne L. Agnew and P. A. McCollum, for their encouragement and instruction during my doctoral studies and while I was an undergraduate. To the Chairman of my committee, Professor K. A. McCollom, I am grateful for his assistance and encouragement during my research.

The National Science Foundation provided financial support during the final two years of my graduate studies for which I gratefully acknowledge.

Finally, to my wife, Lana, I express my warmest appreciation for her encouragement and sacrifice throughout my graduate program. She also is to be thanked for typing this thesis.

TABLE OF CONTENTS

Chapter	Page
I. INTRODUCTION	1
Statement of the Problem.	1
Outline of Solution Methods and Previous Work in the Area.	1
II. DEVELOPMENT OF THE SYSTEM MODEL.	4
Introduction.	4
Inertial Navigation Systems	4
Rotation of Coordinate Reference Frame.	5
Basic Inertial Sensors.	7
Interconnection of the Inertial Elements.	9
Velocity Damped Channel	10
Development of the System Error Model	13
III. THE SYSTEM STATE MODEL	15
Introduction.	15
Gyro Drift.	15
Reference Velocity Noise.	16
System State Model.	17
IV. RECURSIVE SOLUTION OF THE STATE MODEL.	22
General Solution of State Model and the Initial State	22
Recursive State Solution.	23
V. RECURSIVE ESTIMATES.	25
Introduction.	25
Definitions and Notation for Some Conditional Means and Covariances	25
Transition of Estimates	26
Modifications for the Case when σ_v is Unknown	28
VI. APPLICATION OF BAYESIAN LEARNING TO SYSTEM	31
Definitions and Discussion of Bayesian Learning	31
Learning G_B with σ_v Known	33
Learning G_B with σ_v Unknown	35

Chapter	Page
VII. ALGORITHMS FOR COMPUTING \hat{G}_n	40
Computational Procedure for Evaluating \hat{G}_n when σ_v is Known	40
Computational Procedure for Evaluating \hat{G}_n when σ_v is Unknown	43
Summary	44
VIII. EMPIRICAL LEARNING	46
Introduction	46
Empirical Estimate	46
Recursive Empirical Estimate	49
IX. DISCUSSION AND COMPARISON OF ESTIMATION METHODS	52
Introduction	52
Estimating G_B with Known Variance	52
Estimating G_B with Unknown Variance	57
X. SUMMARY AND CONCLUSIONS	62
Summary	62
Conclusions	63
Recommendations for Further Study	63
BIBLIOGRAPHY	65
APPENDIX A. EVALUATING THE TRANSITION MATRIX	67
APPENDIX B. CONDITIONAL EXPECTED VALUES AND RELATIONSHIPS	71
Introduction	71
Expected Value of g_n	71
Variance of g_n	72
Recursive Properties of Conditional Expectations	73
Modifications for the Case of Unknown σ_v	77
APPENDIX C. CONVERGENCE AND STABILITY	79
Introduction	79
Convergence of the Bayesian Estimate	79
Convergence of the Bayesian a posteriori Density Function	82
Stability with the Learning Loop	83
APPENDIX D. THIRD-ORDER LEVELING	84

LIST OF FIGURES

Figure	Page
2.3.1. Rotation of Coordinate Reference Axes.	6
2.4.1. Model of an Accelerometer.	7
2.4.2. Model of a Gyro Including the Gyro Drift	8
2.6.1. Velocity-Aided Channel Model	12
2.7.1. Error Model of System.	12
3.3.1. State Model of Reference Velocity Error.	18
3.4.1. Block Diagram of System State Model with the Learning Loop	18
3.4.3. Diagram of Transformed State Model	21
9.2.1. Effect of Changing Sample Time on \hat{G}_n	53
9.2.2. Effect of Changing Sample Time on $\hat{\sigma}_n^2$	53
9.2.3. Effect of Changing $\hat{\mu}_0$	55
9.2.4. Effect of Changing $\hat{\sigma}_0$	55
9.2.5. Comparison of Bayes (with Known Noise) Variance to Empirical Variance	56
9.3.1. Empirical Variance and Pseudovariance.	59
9.3.2. Simulation Results	60
9.3.3. Effect of Sampling Period on Empirical Variance.	60
D.1. Third-Order Leveling Loop.	85
D.2. Estimate Time Response	85

CHAPTER I

INTRODUCTION

1.1 Statement of the Problem. Inertial navigation systems have taken on a major share of the navigation and guidance of most space vehicles and ballistic missiles as well as many military aircraft and marine vessels. Accurate performance of inertial systems depends not only upon environmental conditions but also upon basic inertial component limitations. Inertial system accuracy is especially sensitive to gyro drift.

In some current military aircraft applications, inertial navigators must be put into operation while airborne, and this can result in significant accuracy degradation unless some method is employed to remove or trim the gyro drift. This condition may become quite severe if the inertial system has been exposed to a low temperature environment prior to operation.

This thesis is concerned with the problem of reducing gyro drift in an inertial navigation system on a moving vehicle. Three solutions to this problem are considered: third-order leveling, Bayesian learning, and empirical estimation.

1.2 Outline of Solution Methods and Previous Work in the Area.

The third-order leveling method, which is presented in Appendix D, represents a standard approach to minimize gyro drift. Since it has been actually implemented on inertial navigators, this method serves as

a basis of comparison for the other methods.

The Bayesian learning techniques discussed in this paper have previously been applied to some problems in the area of pattern recognition (8), (12). Ho and Lee (6) discuss in general the applicability of the Bayesian approach to estimation of control system states under the assumption of Gaussian noise with completely known statistical properties; since their investigation is limited to estimation, generation of a control signal is not discussed.

In a recent book, Aoki (2) presents a general study of optimization and the generation of control signals in a closed loop fashion. For the case of known noise variance, he makes frequent use of Bayes' rule although his control policy is established from dynamic programming considerations. He abandons Bayesian techniques altogether for a minimax approach when he considers the case of an unknown noise variance; he further restricts the unknown variance to be a member of a finite number of known values.

The Bayesian learning technique is used in this paper for learning or estimating the gyro drift for both the case where the noise variance is specified and the case for unknown variance. For the known noise case, it is assumed that both the noise process and the a priori density of the gyro drift are normally distributed. In the latter case, the noise process is assumed normal while the joint a priori density of the gyro drift and the unknown noise variance is assumed to follow a Gaussian-inverted Wishart law. The estimates formed are used in a feedback loop to cancel the unwanted gyro drift.

A survey of recent control system literature will reveal that the Kalman filter approach (7) is almost exclusively being applied to esti-

mation problems similar to the one of this paper. The Kalman method, which is somewhat of a special case of Bayesian learning, is not applicable if the noise variance is unspecified.

The empirical estimation procedure presented in this paper essentially makes use of the sample mean as the basic estimate. Although this technique may lack the mathematical elegance of the Bayesian or the Kalman methods, it allows one to relax some assumptions which may be unrealistic in many applications. Specifically, one does not have to know the density laws for the gyro drift nor of the noise process. The empirical method shares in common with the other two methods the advantage that the estimate can be cast into a recursive form.

The expected value of the squared error between the estimate and the actual gyro drift will be used as the criteria of goodness. The Bayesian estimate is optimal in that it minimizes the mean squared error while the empirical method is suboptimal.

It should be mentioned that the system model is linear. The problem would no doubt be very difficult to solve for a nonlinear system.

CHAPTER II

DEVELOPMENT OF THE SYSTEM MODEL

2.1 Introduction. A brief description of the class of inertial navigation systems to be investigated in this thesis is presented in this chapter. The system error model is developed for use in the succeeding work. Since the treatment here is, of necessity, limited, the reader may want to refer to one of many texts (10), (14) on the subject.

2.2 Inertial Navigation Systems. Inertial navigation implies the direction of a vehicle in the coordinates of inertial space rather than only in the reference frame of the earth or some other body. The term inertial navigation system is generally accepted to mean an assemblage of gyroscopes, accelerometers, and ancillary electromechanical equipment which typically are functionally arranged as follows: Three gyroscopes are mounted on a platform with their input axes mutually orthogonal so as to define a rectangular coordinate frame; associated with these gyros are amplifiers, motors, etc., interconnected to maintain the platform coordinates fixed in space.

A set of platform-mounted accelerometers, each aligned along the axes defined by the gyroscope inputs, sense platform accelerations along these axes; associated with each of these instruments are integrators which ideally provide instantaneous velocity and distance traveled.

Typically the platform on which the inertial instruments are

mounted is suspended by a gimbal system to provide angular isolation from the environment. The gyros sense angular motion of the platform and provide signals to platform gimbal servos to maintain desired platform orientation.

The above assembly of equipment is truly an inertially referenced system due to inherent properties of the instruments. That is, the gyroscopes sense angular changes with respect to the "stars" and the accelerometers measure absolute linear accelerations. The system acts to resolve an acceleration into components along the inertial frame.

For relatively short periods of operation, less than four or five hours, the three axes defined by the inertial sensors can be considered to be independent of each other so long as there are no large errors. Thus one can consider the computations associated with each axis individually if he neglects crosscoupling between the axes.

2.3 Rotation of Coordinate Reference Frame. Inertial navigation systems used for navigation over the surface of the earth are called cruise inertial systems. Most of these are mechanized to operate with their respective axes oriented in the direction of east, north, and up and are sometimes referred to as local-level, north-oriented systems. Such a system is said to be aligned when the proper axis (azimuth) coincides with the vertical vector (local-level) and the appropriate axis is pointed north (north-oriented). The system to be discussed in this thesis is of this type.

As a local-level system is moved from along some path over the surface of the earth, control signals are generated to maintain a vertical azimuth axis. This control signal is required since an inertial

system does not have the earth for a reference.

Consider, for example, the situation depicted in Figure 2.3.1. The vertical and east axes are labeled while the north axis is assumed to point into the plane of the paper. Suppose that this coordinate frame, assumed to be locally-leveled initially, is carried an angular distance east ϕ_a ; then, in order to maintain the U-axis vertical, the coordinate axes must be rotated by the same angle ϕ_a . To maintain the proper orientation continuously, the coordinate reference frame needs to be rotated at an angular rate $\dot{\phi}_a$. It should be noted that the rotation rate $\dot{\phi}_a$, being an angular velocity, is not measured by the sensors and it must therefore be provided by computation or mechanized in a manner to be discussed below.

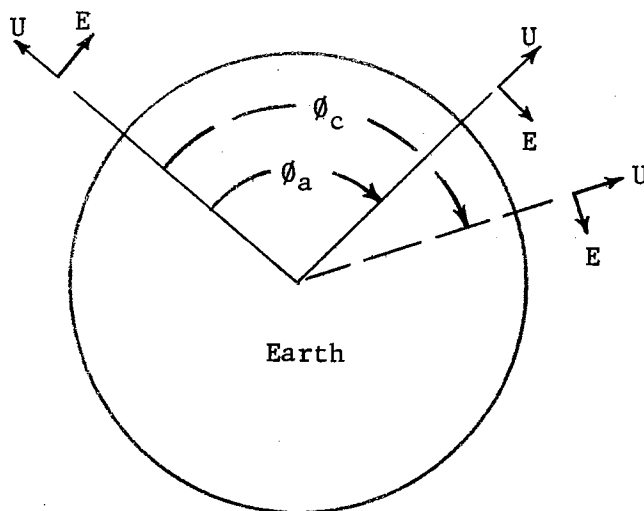


Figure 2.3.1. Rotation of Coordinate Reference Axes

Also illustrated in Figure 2.3.1 is the effect of an error in computation of the angle ϕ_a . If the system makes an error in the compu-

tation of $\dot{\phi}_a$ (or $\ddot{\phi}_a$) there will be an error in the orientation of the axes. That is, if the system provides a computed angular distance ϕ_c while the actual angular distance traveled is ϕ_a , there will result an error angle $\phi_e = \phi_c - \phi_a$ about the north axis of the coordinate frame. Or, in terms of angular rates, $\dot{\phi}_e = \dot{\phi}_c - \dot{\phi}_a$.

2.4 Basic Inertial Sensors. The two basic types of sensors used in an inertial navigation system are accelerometers and gyroscopes and, in a complete system, there are three of each. It should be added that the functions of two sensors are sometimes combined in a single instrument; however, functionally they can be regarded as separate units.

An accelerometer model, sufficient for the purposes of this thesis, is presented in Figure 2.4.1. The device is assumed to be a transducer which converts the net acceleration input to a proportional voltage output. The net acceleration illustrated is the sum of the actual acceleration a_a and the apparent acceleration due to gravitation effects a_g ; when a local-leveled system is properly aligned, that is, to the local vertical, the north- and the east-axis accelerometers will sense no gravitational acceleration but the azimuth-axis accelerometer will measure g plus any actual upward accelerations.

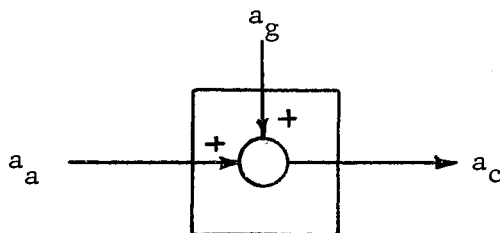


Figure 2.4.1. Model of an Accelerometer

The accelerometer is very carefully designed so that it is sensitive to linear accelerations only in the direction of its defined axis. For the north-oriented, local-level system, one accelerometer is mounted with its sensitive axis pointed in a north-south direction; an identical instrument is pointed east-west. A third could be mounted with its sensitive axis in the vertical direction but often this unit is omitted.

The gyroscopes, typically of the integrating type, are used as sensors in a so-called platform servo loop to maintain proper coordinate orientation. A description of the details of platform servo loops is too lengthy to be included here. It suffices for the purpose here to state that one can achieve rotation of the coordinate frame by applying a control signal to the appropriate platform servo and that the servo acts, with the gyroscope as a sensor, to keep the reference coordinates stabilized.

Rotation of the reference coordinates at an angular rate $\dot{\phi}_d$ can be accomplished by applying a signal to the platform servo. Over a time of observation t the net angular rotation will be given by

$$\phi_c(t) = \int_0^t \dot{\phi}_d(x) dx. \quad (2.4.1)$$

Therefore the model presented in Figure 2.4.2 will be used for the gyroscope-platform servo which will be hereafter referred to simply as the gyro.

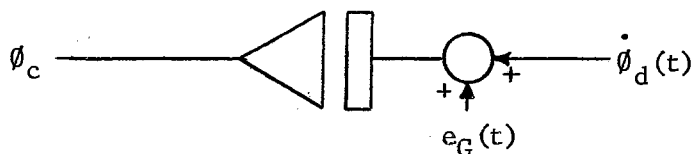


Figure 2.4.2. Model of a Gyro Including the Gyro Drift

One will note in Figure 2.4.2 that an additional signal $e_G(t)$ has been included as an input to the integrator. This signal represents the so-called gyro drift which is assumed to be a normal stochastic process. Unwanted torques produced in the gyroscope cause its characteristics to change or drift randomly from the desired operating condition. These spurious drifts can be grouped as:

- (a) constant drifts [mean value of $e_G(t)$] and
- (b) variational drifts [variance of $e_G(t)$].

These drifts will be discussed further in the next chapter.

2.5 Interconnection of the Inertial Elements. The use made of the gyro which has its sensitive axis vertical (the azimuth-gyro) is different from east- and north-gyros (the level gyros) in that it is normally operated in an open loop manner with no corrective input signals being applied. The azimuth gyro simply performs the function of maintaining proper orientation of the coordinate axes about the vertical.

Since crosscoupling between the three axes is being ignored, the description of the mechanization for each axis can be discussed individually. With the exception of some corrective input signals applied to compensate for the earth turning rate and Coriolis effects, the functional description of the mechanization for each of the level axes will be identical.

The (basic, unaided) east channel functionally includes the following components: the east-axis accelerometer, two integrators, the north-axis gyro, and a gain constant R^{-1} . The net measured east acceleration a_c is integrated to give computed velocity v_c in the east-

ward direction. The resulting velocity is integrated to give computed distance traveled. Computed velocity is also used to maintain the platform level-orientation through rotation of the coordinate frame about the north axis by applying $v_c R^{-1}$ to the north gyro.

Similarly, the north channel includes the north-accelerometer, two integrators, the east-gyro and the gain constant R^{-1} which provide analogous functions.

2.6 Velocity Damped Channel. The accuracy of an inertial navigation system is excellent for a short period of operation but decreases with increasing operating time. The long term accuracy of a doppler radar, conversely, is quite good yet it tends to be noisy. Combining the two systems has been found to give a low-noise velocity measurement with good accuracy characteristics for large operating times.

This thesis is specifically limited to the doppler radar aided channel, a functional block diagram of which is presented in Figure 2.6.1. The following list describes the symbols and notation employed:

- v_a = actual velocity
- v_c = computed velocity
- v_r = reference velocity provided by the doppler radar
- e_v = error in the doppler radar reference velocity
- d_c = computed linear distance
- ϕ_a = actual angular distance traveled
- ϕ_c = computed angular distance traveled
- $\phi_e = \phi_c - \phi_a$ = error in platform level
- a_a = actual acceleration (east)

a_g = gravitation acceleration sensed (caused by error in level)

G_B = gyro drift

g = gravitational acceleration (32.2 feet/sec^2)

R = earth radius (2.09×10^7 feet)

$K_1 = .02$

$K_2 = 100$

Some of the terms in the above list have been previously discussed and the remainder will now be described to complete a functional description of the model under investigation. The term ϕ_e represents the difference between actual angular distance traveled and computed angular distance. This term arises from the fact that the system actually rotates the platform through angle ϕ_c in an attempt to keep the coordinate frame level rather than through the proper angle ϕ_a ; the tilt angle ϕ_e is the amount of error between the east-axis attitude and the actual axis level.

When ϕ_e is zero, the east accelerometer will sense only the actual east acceleration a_a . However, a non-zero tilt angle will result in an additional acceleration due to gravity of

$$a_g = g \sin \phi_e. \quad (2.6.1)$$

The angle ϕ_e is assumed to be small enough (less than one milliradian) to allow the small angle approximation to be valid; therefore

$$a_g = g \phi_e. \quad (2.6.2)$$

The net measured acceleration is therefore given by

$$a_c = a_a - g \phi_e \quad (2.6.3)$$

where the minus sign appears because of the sign convention of the

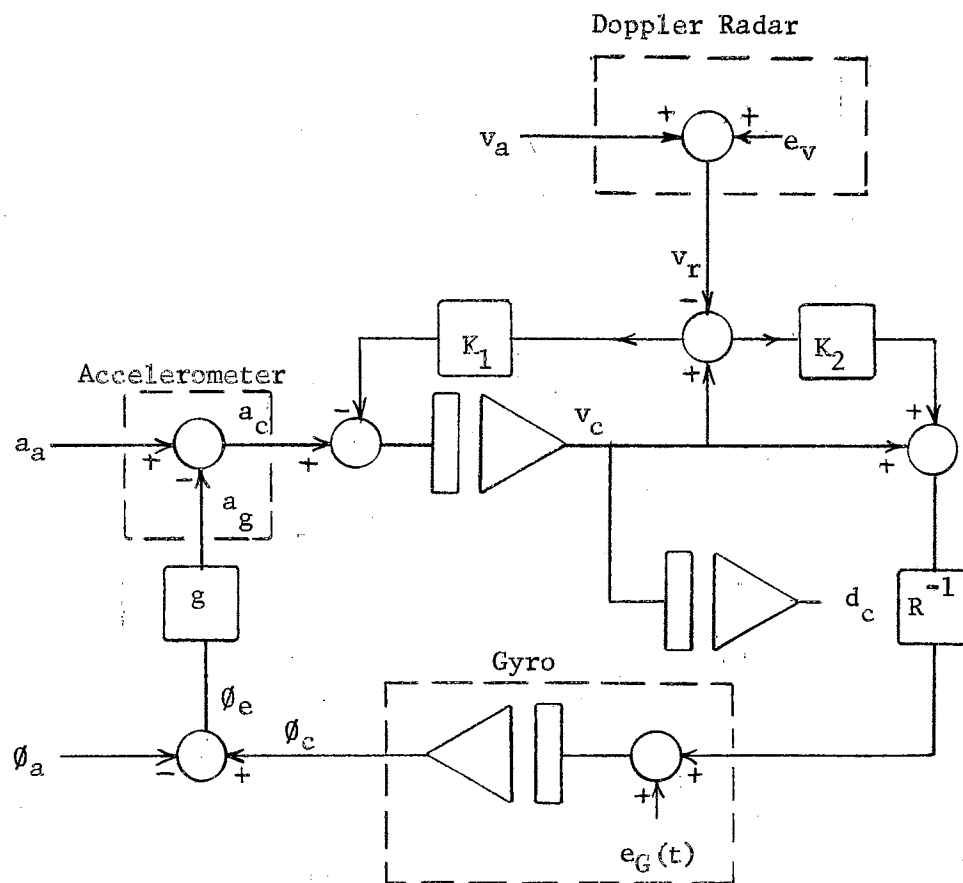


Figure 2.6.1. Velocity-Aided Channel Model

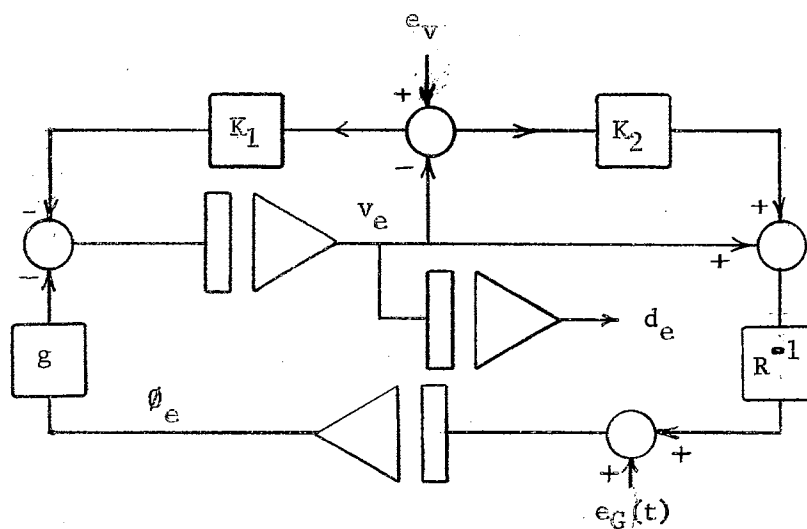


Figure 2.7.1. Error Model of System

assumed coordinate system.

The gain constants K_1 and K_2 were arbitrarily chosen as .02 and 100 respectively to give typical platform dynamic characteristics. With this selection of parameters, the system has a time constant of 100 seconds and a damping ratio of about 0.8.

2.7 Development of the System Error Model. The system model presented in Figure 2.6.1 describes the overall system behavior. However, it is desirable to have a different model of the system which describes only the behavior of system errors as functions of time. This model can be readily obtained by defining velocity error v_e and distance error d_e with the following equations:

$$v_c = v_a + v_e \quad (2.7.1)$$

$$d_c = d_a + d_e \quad (2.7.2)$$

where d_a is the actual distance traveled; also one can show

$$v_e = \dot{d}_e \quad (2.7.3)$$

$$v_e = R \dot{\theta}_e \quad (2.7.4)$$

By considering the physical quantities involved, one can establish

$$a_a = \dot{v}_a \quad (2.7.5)$$

$$v_a = R \dot{\theta}_a \quad (2.7.6)$$

$$v_a = \dot{d}_a \quad (2.7.7)$$

The system of differential equations describing the behavior of the model of Figure 2.6.1 is

$$\dot{v}_c = a_a + g\theta_e - K_1 v_c + K_1 (v_a + e_v) \quad (2.7.8)$$

$$\dot{\theta}_c = G_B + [(1 + K_2)/R] v_c - K_2 (v_a + e_v)/R \quad (2.7.9)$$

$$\dot{d}_c = v_c. \quad (2.7.10)$$

Solving Equations 2.7.1 through 2.7.10 for the error terms gives the following set of differential equations:

$$\dot{v}_e = g\phi_e - K_1 v_e + K_1 e_v \quad (2.7.11)$$

$$\dot{\phi}_e = G_B + [(1 + K_2)/R]v_e - K_2 e_v/R \quad (2.7.12)$$

$$\dot{d}_e = v_e. \quad (2.7.13)$$

It is especially important to note that this set of differential equation models the system errors in terms of the error sources G_B and e_v and that these equations are independent of true system values. In other words, the solution of this set of differential equations describes how errors propagate as functions of time and error source inputs and not as functions of a_a , v_a and ϕ_a . A block diagram of this error model is presented in Figure 2.7.1.

In the analysis which is to follow, use will be made of the signal $v_e - e_v$; the reader will note this signal per se is not available for measurement since it is the difference of two nonobservable quantities. However $v_c - v_r$ is a physically measurable quantity and since

$$v_c - v_r = v_e - e_v \quad (2.7.14)$$

the nonobservable property is circumvented.

CHAPTER III

THE SYSTEM STATE MODEL

3.1 Introduction. The functional model of the system to be investigated in this thesis was developed in the previous chapter. The variables v_e and ϕ_e are time functions which physically represent instantaneous velocity error and tilt error respectively. In this chapter the input error processes are discussed and a state model of the system is developed.

3.2 Gyro Drift. There are two random inputs to the system: gyro drift $e_G(t)$ and reference velocity error $e_v(t)$, both of which are assumed to be normal random processes. Present day high quality gyros have small variations about their mean values; standard deviations less than .01 degrees per hour are not uncommon. Moreover, the rate at which the gyro drifts about its mean, as measured by the so called correlation time, is quite slow (4), (5). Thus the effect on instantaneous velocity error by the variations of gyro drift is quite small in comparison to effects caused by other error sources such as $e_v(t)$. It will therefore be assumed that the gyro drift $e_G(t)$ is a constant random process.

The mean value G_B of the gyro drift or gyro bias is assumed to be a random variable. If an inertial navigation system is pre-aligned before use on a stationary base, the gyro biases can be essentially canceled by one of several trim techniques (14).

However, under many current military practices, the system is put into operation while airborne and ground alignment techniques are therefore not available. If the system is started after a prolonged period of exposure at low temperature, the value of G_B can be comparatively large, typically about two degrees per hour (14). In this thesis, the probability density function of G_B is assumed to be given by

$$f_{G_B}(z) = \frac{1}{\sqrt{2\pi}\hat{\sigma}_0} \exp \left[-\frac{(z - \hat{\mu}_0)^2}{2\hat{\sigma}_0^2} \right] . \quad (3.2.1)$$

The mean $\hat{\mu}_0$ and variance $\hat{\sigma}_0^2$ in Equation 3.2.1 are assumed to be known.

3.3 Reference Velocity Noise. The second error source to be discussed is reference velocity noise $e_v(t)$ which is assumed to be associated with an airborne doppler radar. As is customary, it will be assumed that $e_v(t)$ is a normal random process which is band-limited white noise. Thus at any given time t , the probability density function of $e_v(t)$ is assumed to be

$$f_{e_v(t)}(v) = \frac{1}{\sqrt{2\pi}\sigma_v} \exp \left[-\frac{v^2}{2\sigma_v^2} \right] \quad (3.3.1)$$

and the power spectrum of $e_v(t)$ is, by assumption,

$$S_{vv}(w) = \frac{2b\sigma_v^2}{w^2 + b^2} .$$

The following values are assumed for the standard deviation and corner frequency of the power spectrum:

$$\sigma_v = 1 \text{ foot/second}$$

$$b = 1 \text{ radian/second}$$

Elsewhere in this thesis an assumption will be made that σ_v is not the above value but is some unknown number following a known probability

density law.

It is desired to have a state model representation of the reference velocity error process. This can be obtained by first modeling the process as unity white noise passed through a shaping filter and then writing the state model for the shaping filter. The shaping filter has a transfer function given by

$$H(s) = \frac{\sqrt{2b\sigma_v}}{s + b}.$$

Therefore the reference velocity error process state model is as illustrated in Figure 3.3.1. The process $v(t)$ is assumed to be a normal, white noise stochastic process with the following respective probability density function and autocorrelation function:

$$f_{v(t)}(v) = \frac{1}{\sqrt{2\pi}} \exp\left[-\frac{v^2}{2}\right] \quad (3.3.2)$$

$$R_{vv}(\tau) = \delta(\tau), \quad (3.3.3)$$

where $\delta(\cdot)$ is the delta function.

3.4. System State Model. The complete state model of the system with the learning loop is presented in Figure 3.4.1. The procedure for learning will be discussed below. Represented on the diagram are the system states $x_1(t)$, $x_2(t)$, and $x_3(t)$ which are respectively velocity error, tilt error, and reference velocity error. Inputs to the system are gyro drift mean or bias G_B and the unity white-noise process $v(t)$.

The learning loop performs the function of providing an optimum estimate \hat{G} of G_B , given a time sequence of measurements $y(T)$, $y(2T)$, ..., and canceling G_B by subtracting \hat{G} . The procedure of estimating

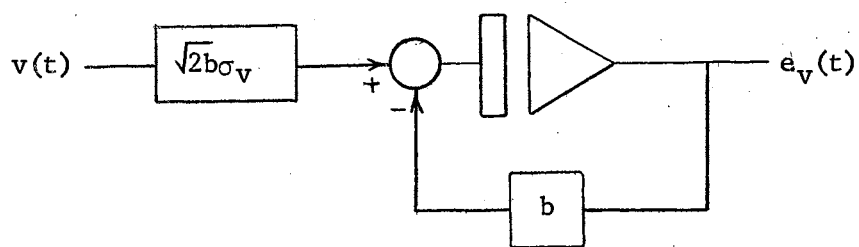


Figure 3.3.1. State Model of Reference Velocity Error

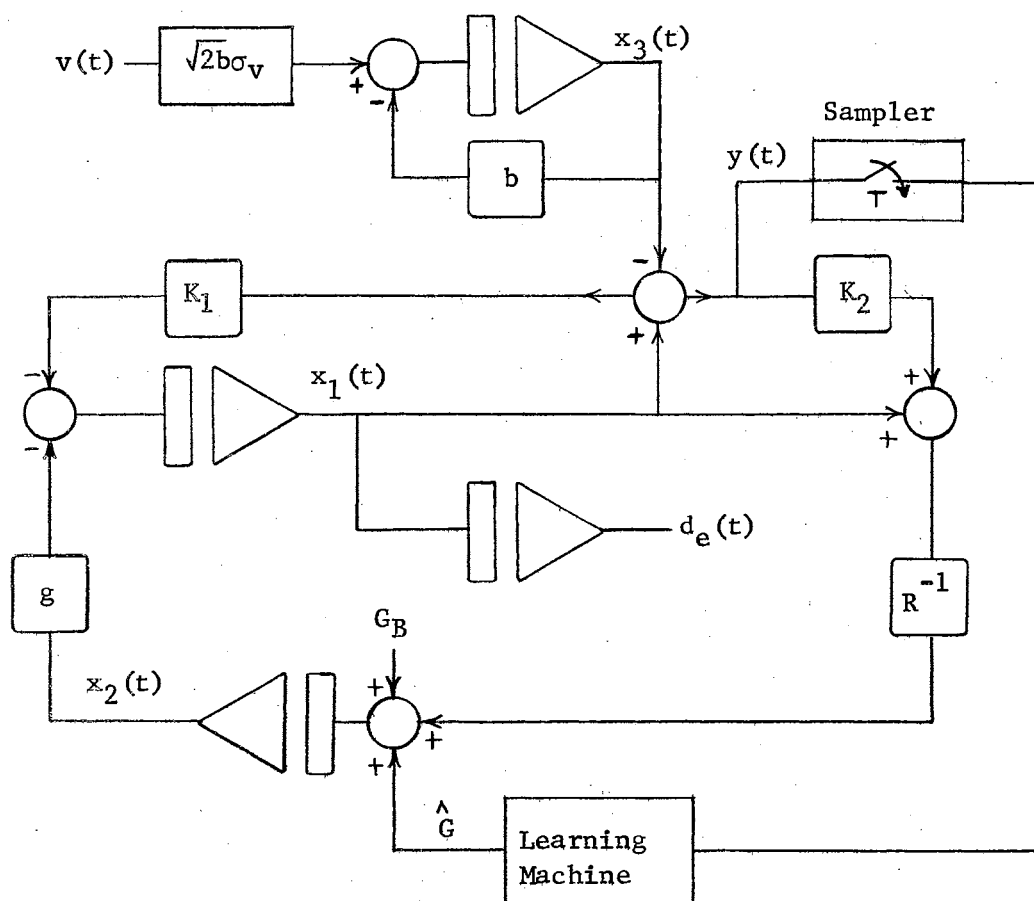


Figure 3.4.1. Block Diagram of System State Model with the Learning Loop

G_B will be referred to as learning, a terminology carried over from pattern recognition.

It will be shown that the solution for \hat{G} can be expressed recursively, that is, as each new measurement is obtained, the previous estimate of G_B can be revised to reflect the additional information. This minimizes the storage requirement for the mechanization of the estimator or learning machine in that only the previous estimate has to be stored rather than the entire history of measurements.

Mathematically, the state model can be expressed as the following set of equations:

$$\begin{bmatrix} \dot{x}_1(t) \\ \dot{x}_2(t) \\ \dot{x}_3(t) \end{bmatrix} = \begin{bmatrix} -K_1 & -g & K_1 \\ (1 + K_2)/R & 0 & -K_2/R \\ 0 & 0 & -b \end{bmatrix} \begin{bmatrix} x_1(t) \\ x_2(t) \\ x_3(t) \end{bmatrix} + \begin{bmatrix} 0 & 0 \\ 1 & 0 \\ 0 & \sigma_v \sqrt{2b} \end{bmatrix} \begin{bmatrix} G_B - \hat{G} \\ v(t) \end{bmatrix}$$

$$y(t) = \begin{bmatrix} 1 & 0 & -1 \end{bmatrix} \begin{bmatrix} x_1(t) \\ x_2(t) \\ x_3(t) \end{bmatrix}$$

Or, using the vector-matrix symbolization,

$$\dot{\underline{x}}(t) = \underline{A}' \underline{x}(t) + \underline{B}' \underline{v}(t)$$

$$y(t) = \underline{C}' \underline{x}(t)$$

where

$$\underline{x}(t) = \begin{bmatrix} x_1(t) \\ x_2(t) \\ x_3(t) \end{bmatrix}, \quad \underline{v}(t) = \begin{bmatrix} G_B - \hat{G} \\ v(t) \end{bmatrix}$$

and \underline{A}' , \underline{B}' , and \underline{C}' are the respective coefficient matrices.

The measurement $y(t)$ is the difference between the two states

$x_1(t)$ and $x_3(t)$. Some simplification in subsequent notation for recursive estimates will be realized by the following change of variables:

$$\underline{z}(t) = \begin{bmatrix} z_1(t) \\ z_2(t) \\ z_3(t) \end{bmatrix} = \begin{bmatrix} 1 & 0 & 0 \\ 0 & 1 & 0 \\ 1 & 0 & -1 \end{bmatrix} \begin{bmatrix} x_1(t) \\ x_2(t) \\ x_3(t) \end{bmatrix} = \underline{M} \underline{x}(t) .$$

Effecting this change of variables results in the following system of equations:

$$\dot{\underline{z}}(t) = \underline{A} \underline{z}(t) + \underline{B} \underline{v}(t)$$

$$y(t) = \underline{C} \underline{z}(t)$$

where

$$\underline{A} = \underline{M} \underline{A}' \underline{M}^{-1} = \begin{bmatrix} 0 & -g & -K_1 \\ 1/R & 0 & K_2/R \\ b & -g & -K_1 - b \end{bmatrix}$$

$$\underline{B} = \underline{M} \underline{B}' = \begin{bmatrix} 0 & 0 \\ 1 & 0 \\ 0 & -\sigma_v \sqrt{2b} \end{bmatrix}$$

$$\underline{C} = \underline{C}' \underline{M}^{-1} = \begin{bmatrix} 0 & 0 & 1 \end{bmatrix}$$

A block diagram of the system in terms of the transformed state variables is presented in Figure 3.4.2.

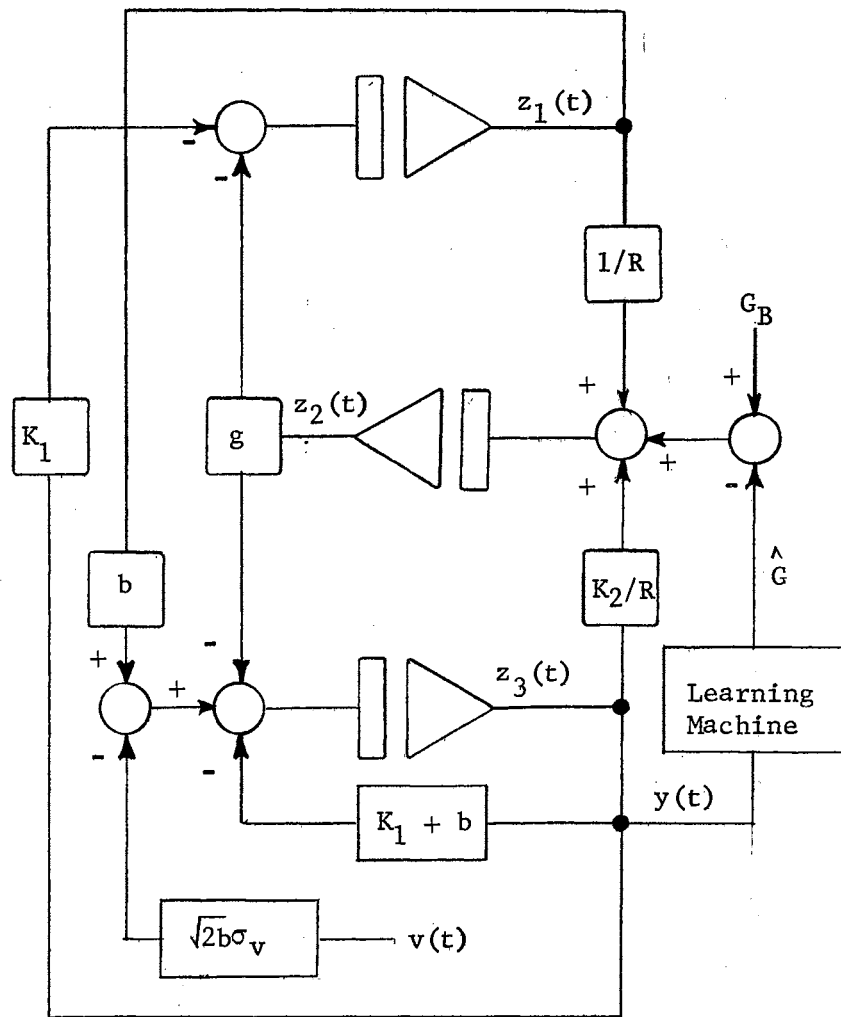


Figure 3.4.2. Diagram of Transformed State Model

CHAPTER IV

RECURSIVE SOLUTION OF THE STATE MODEL

4.1 General Solution of State Model and the Initial State. The usual form of the state solution of the model

$$\dot{\underline{z}} = \underline{A} \underline{z} + \underline{B} \underline{v} \quad (4.1.1)$$

$$\underline{y} = \underline{C} \underline{z}$$

in terms of the initial vector $\underline{z}(t_0)$ and the transition matrix $\underline{\phi}(t) = \exp(\underline{A}t)$ is given by (9)

$$\begin{aligned} \underline{z}(t) &= \underline{\phi}(t - t_0) \underline{z}(t_0) + \int_{t_0}^t \underline{\phi}(t - x) \underline{B} \underline{v}(x) dx, \quad t \geq t_0 \\ \underline{y}(t) &= \underline{C} \underline{z}(t), \quad t \geq t_0. \end{aligned} \quad (4.1.2)$$

The transition matrix is discussed in Appendix A.

A more useful form of Equation 4.1.2 can be obtained by defining the two vectors

$$\underline{B}_1 = \begin{bmatrix} 0 \\ 1 \\ 0 \end{bmatrix}, \quad \underline{B}_2 = \begin{bmatrix} 0 \\ 0 \\ 1 \end{bmatrix} \quad (4.1.3)$$

which will result in the following equation:

$$\begin{aligned} \underline{z}(t) &= \underline{\phi}(t - t_0) \underline{z}(t_0) + \int_{t_0}^t \underline{\phi}(t - x) \underline{B}_1 (\underline{G}_B - \hat{\underline{G}}) dx \\ &\quad - \sqrt{2b}\sigma_v \int_{t_0}^t \underline{\phi}(t - x) \underline{B}_2 v(x) dx. \end{aligned} \quad (4.1.4)$$

To establish initial conditions for the system, it will be

assumed that the input random processes have been applied long before (i.e., when $t_0 = -\infty$) the learning procedure is initiated. The initial time for starting the learning process will be chosen when time is zero; therefore \hat{G} is zero for negative time. It is obvious from the form of the transition matrix, Equation A.7, that $\underline{\phi}(\infty) = \underline{0}$; hence the initial state vector is found from Equation 4.1.3 to be

$$\underline{z}(0) = G_B \int_{-\infty}^0 \underline{\phi}(-x) \underline{B}_1 dx - \sqrt{2} b_{\sigma_v} \int_{-\infty}^0 \underline{\phi}(-x) \underline{B}_2 v(x) dx \quad (4.1.5)$$

where G_B has been removed from the integrand since it is a constant random process.

4.2 Recursive State Solution. The compensating signal \hat{G} is computed as each measurement in the time sequence $y(T)$, $y(2T)$, ... is obtained where no measurement is made at the initial instant. The initial estimate of G_B will be denoted by \hat{G}_0 and the succeeding estimates will be denoted by \hat{G}_n . The estimate \hat{G} is therefore a piecewise continuous (step) function with its discontinuities occurring at the sampling instants; hence, the form of \hat{G} is

$$\hat{G} = \hat{G}_n, \quad nT \leq t < (n+1)T. \quad (4.2.1)$$

Since the basic nature of the learning system is discrete, it is desirable to have a solution which explicitly describes the behavior of the system at the sampling instants. This recursive form of the solution can be simply obtained by substituting Equation 4.2.1 into Equation 4.1.4 and evaluating the result at the sampling times to get

$$\begin{aligned} \underline{z}(nT + T) = & \underline{\phi}(T) \underline{z}(nT) + (G_B - \hat{G}_n) \int_{nT}^{nT+T} \underline{\phi}(nT + T - x) \underline{B}_1 dx \\ & - \sqrt{2b\sigma_v} \int_{nT}^{nT+T} \underline{\phi}(nT + T - x) \underline{B}_2 v(x) dx, \quad n \geq 0 \end{aligned} \quad (4.2.2)$$

where $(G_B - \hat{G}_n)$ appears outside the integral sign since it is constant over the time of integration.

It can be shown, by a simple change of integration variable, that the integral in the second term is the same for all non-negative integers n which can be used to simplify the appearance of Equation 4.2.2. Further simplification can be achieved by using the definition

$$\underline{g}_{n+1} = -\sqrt{2b\sigma_v} \int_{nT}^{nT+T} \underline{\phi}(nT + T - x) \underline{B}_2 v(x) dx, \quad n \geq 0 \quad (4.2.3)$$

to obtain the desired result

$$\underline{z}(nT + T) = \underline{\phi}(T) \underline{z}(nT) + (G_B - \hat{G}_n) \underline{\theta} + \underline{g}_{n+1}, \quad n \geq 0 \quad (4.2.4)$$

where

$$\underline{\theta} = \int_0^T \underline{\phi}(T - x) \underline{B}_1 dx. \quad (4.2.5)$$

The vectors $\underline{\theta}$ and \underline{g}_n are discussed in Appendices A and B respectively.

Similarly, one can define

$$\underline{\theta}_0 = \int_{-\infty}^0 \underline{\phi}(-x) \underline{B}_1 dx \quad (4.2.6)$$

and

$$\underline{g}_0 = -\sqrt{2b\sigma_v} \int_{-\infty}^0 \underline{\phi}(-x) \underline{B}_2 v(x) dx \quad (4.2.7)$$

to have an expression for Equation 4.1.5 which is analogous to Equation 4.2.4.

$$\underline{z}(0) = \underline{\theta}_0 G_B + \underline{g}_0. \quad (4.2.8)$$

CHAPTER V

RECURSIVE ESTIMATES

5.1 Introduction. In the next chapter, the learning algorithms will be derived from a Bayesian formulation. However, to use Baye's rule, it will be necessary to have the density functions which describe the processes. In this chapter, a useful chain of recursive relations will be derived for the various conditional means and covariance matrices. Frequent reference to the Appendix will be made where several properties are developed.

5.2 Definitions and Notation for Some Conditional Means and Covariances. Using the notation $\underline{y}(nT) = \{y(T), \dots, y(nT)\}$, the following definitions, which are strongly motivated by the work of Kalman (7), will be made:

$$\hat{\underline{z}}_0 = E[\underline{z}(0) | G_B] \quad (5.2.1)$$

$$\hat{\underline{z}}_n = E[\underline{z}(nT) | G_B, \underline{y}(nT)], \quad n \geq 1 \quad (5.2.2)$$

$$\underline{e}_n = \underline{z}(nT) - \hat{\underline{z}}_n, \quad n \geq 0 \quad (5.2.3)$$

$$\underline{P}_0 = E(\underline{e}_0 \underline{e}_0^T | G_B) \quad (5.2.4)$$

$$\underline{P}_n = E[(\underline{e}_n \underline{e}_n^T | G_B, \underline{y}(nT)], \quad n \geq 1 \quad (5.2.5)$$

$$\hat{\underline{z}}_1' = E[\underline{z}(T) | G_B] \quad (5.2.6)$$

$$\hat{\underline{z}}_n' = E[\underline{z}(nT) | G_B, \underline{y}(nT - T)], \quad n \geq 2 \quad (5.2.7)$$

$$\underline{e}_n' = \underline{z}(nT) - \hat{\underline{z}}_n', \quad n \geq 1 \quad (5.2.8)$$

$$\underline{P}_1^* = E(\underline{e}_1' \underline{e}_1'^T | G_B) \quad (5.2.9)$$

$$\underline{P}_n^* = E[\underline{e}_n \underline{e}_n^T | G_B, \underline{y}(nT - T)], \quad n \geq 2 \quad (5.2.10)$$

Also it will prove useful to incorporate the following notational conveniences:

$$\underline{\hat{z}}_n = \begin{bmatrix} \hat{z}_1(n) \\ \hat{z}_2(n) \\ \hat{z}_3(n) \end{bmatrix}, \quad \underline{\hat{z}}'_n = \begin{bmatrix} \hat{z}'_1(n) \\ \hat{z}'_2(n) \\ \hat{z}'_3(n) \end{bmatrix} \quad (5.2.11)$$

5.3 Transition of Estimates. The first pair of transition equations are contained in the following properties:

Property B.4.5. For $n \geq 1$, $\underline{\hat{z}}'_n = \underline{\phi}(T) \underline{\hat{z}}'_{n-1} + (G_B - \hat{G}_{n-1}) \underline{\theta}$.

Property B.4.6. For $n \geq 1$, $\underline{P}_n^* = \underline{\phi}(T) \underline{P}_{n-1} \underline{\phi}^T(T) + \underline{H}$.

\underline{H} is given by Equation B.3.5. These properties, which are derived in Appendix B, describe the transitional relations of $\underline{\hat{z}}'_{n-1}$ to $\underline{\hat{z}}'_n$ and \underline{P}_{n-1} to \underline{P}_n^* . To complete the recursive chain, the relationship of $\underline{\hat{z}}'_n$ to $\underline{\hat{z}}_n$ and \underline{P}_n^* to \underline{P}_n will be established.

It was shown in Appendix B, Property B.4.1, that both $\underline{z}(nT)$ and $\underline{y}(nT)$ are linear combinations of the normal random variables G_B, g_0, \dots, g_n . Therefore $\underline{z}(nT), G_B$, and $\underline{y}(nT - T)$ are jointly normal and it follows that the density function of $\underline{z}(nT)$, conditioned by G_B and $\underline{y}(nT - T)$, is normal (11). The mean vector and covariance matrix of this density function are given by Equations 5.2.2 and 5.2.5.

Letting $\underline{y}_n = \{y_1, \dots, y_n\}$, one has

$$f_{\underline{z}(nT) | G_B, \underline{y}(nT - T)}(\underline{x} | \underline{z}, \underline{y}_{n-1}) = \left(\frac{1}{2\pi} \right)^{3/2} \frac{1}{|\underline{P}_n^*|^{1/2}} \exp[-(\underline{x} - \underline{\hat{z}}'_n)^T \underline{P}_n^{*-1} (\underline{x} - \underline{\hat{z}}'_n) / 2]. \quad (5.3.1)$$

The matrix \underline{P}_n^* has an inverse since it is positive definite. However, the matrix \underline{P}_n is not positive definite since it has a row and column of zeros. This follows from Equation 5.2.2 and the fact that

$$y(nT) = \underline{C} \underline{z}(nT) = z_3(nT) \quad (5.3.2)$$

which, together, imply

$$\hat{z}_3(n) = y(nT), \quad n \geq 1. \quad (5.3.3)$$

Moreover, for $i = 1, 2$, or 3 ,

$$\begin{aligned} E\{[z_i(nT) - \hat{z}_i(n)][z_3(nT) - \hat{z}_3(n)]^T | G_{B,y}(nT)\} \\ = 0, \quad n \geq 1, \end{aligned} \quad (5.3.4)$$

Hence the \underline{P}_n matrix has the form

$$\underline{P}_n = \begin{bmatrix} \underline{Q}_n & \underline{0} \\ \underline{0}^T & 0 \end{bmatrix} \quad (5.3.5)$$

where \underline{Q}_n is a 2×2 matrix defined by Equation 5.3.5.

The vectors \underline{q}_n and $\hat{\underline{q}}_n$ will be defined as

$$\underline{q}_n = \begin{bmatrix} z_1(nT) \\ z_2(nT) \end{bmatrix}, \quad \hat{\underline{q}}_n = \begin{bmatrix} \hat{z}_1(n) \\ \hat{z}_2(n) \end{bmatrix}. \quad (5.3.6)$$

The covariance matrix \underline{Q}_n and mean vector $\hat{\underline{q}}_n$ can be computed from \underline{P}_n^* and $\hat{\underline{z}}_n$ using the equation

$$f_{\underline{q}_n | G_{B,y}(nT)} = \frac{f_{\underline{z}(nT) | G_{B,y}(nT - T)}}{f_{z_3(nT) | G_{B,y}(nT - T)}} \quad (5.3.7)$$

which follows from Equation 5.3.2. Since both density functions on the right hand side of Equation 5.3.7 are normal, the conditional density function on the left hand side is also normal; hence

$$f_{\underline{q}_n | G_{B, \underline{y}}(nT)}(\underline{q} | z, \underline{y}_n) = \frac{1}{2\pi} \left(\frac{1}{|Q_n|} \right)^{1/2} \exp[-(\underline{q} - \hat{\underline{q}}_n)^T Q_n^{-1} (\underline{q} - \hat{\underline{q}}_n) / 2]. \quad (5.3.8)$$

The density function in the numerator of Equation 5.3.7 is given by Equation 5.3.1.

The following notation will be introduced to carry out the computation of Q_n and $\hat{\underline{q}}_n$:

$$Q_n = [q_{ij}(n)] \quad (5.3.9)$$

$$\underline{p}_n^* = [p_{ij}(n)]. \quad (5.3.10)$$

Using Equation 5.3.10, the denominator of Equation 5.3.7 can be written

$$f_{z_3(nT) | G_{B, \underline{y}}(nT - T)}(y_n | z, \underline{y}_{n-1}) = \left(\frac{1}{2\pi p_{33}(n)} \right)^{1/2} \exp\left\{ -[y_n - \hat{z}_3^1(n)]^2 / 2p_{33}(n) \right\}. \quad (5.3.11)$$

Substitution of Equations 5.3.1, 5.3.8, and 5.3.11 into Equation 5.3.7 and using Equations 5.3.9 and 5.3.10 will give the following result:

$$Q_n^T = \begin{bmatrix} p_{11}(n) - p_{13}^2(n)/p_{33}(n) & p_{12}(n) - p_{13}(n)p_{23}(n)/p_{33}(n) \\ p_{12}(n) - p_{13}(n)p_{23}(n)/p_{33}(n) & p_{22}(n) - p_{23}^2(n)/p_{33}(n) \end{bmatrix} \quad (5.3.12)$$

$$\underline{q}_n = \begin{bmatrix} \hat{z}_1^1(n) + p_{13}(n)[y_n - \hat{z}_3^1(n)]/p_{33}(n) \\ \hat{z}_2^1(n) + p_{23}(n)[y_n - \hat{z}_3^1(n)]/p_{33}(n) \end{bmatrix} \quad (5.3.13)$$

5.4 Modifications for the Case when σ_v is Unknown. The preceding portion of this thesis carried the assumption that σ_v was a

known value. In this section, this assumption is not made, and σ_v^2 will be treated, analogous to G_B , as a random variable; specifically, the random variable p will be defined as

$$p = 1/\sigma_v^2. \quad (5.4.1)$$

Most of the material presented before this section will not be affected and the modifications to be made will be minor. It can be seen that the results will be the same; only some of the interpretations and definitions will be altered.

The basic difference stems from the expression for the noise convolution term \underline{g}_n which, using Equation 5.4.1, is written

$$\underline{g}_0 = (\sqrt{2b}/p) \int_{-\infty}^0 \underline{\phi}(-x) \underline{B}_2 v(x) dx \quad (5.4.2)$$

$$\underline{g}_n = (\sqrt{2b}/p) \int_{nT-T}^{nT} \underline{\phi}(nT - x) \underline{B}_2 v(x) dx, \quad n \geq 1. \quad (5.4.3)$$

Also all of the various conditional expectations are interpreted to be conditioned also by p ; for example $E(\underline{g}_n \underline{g}_n^T | p)$, $E[\underline{z}(n) | p, G_B, \underline{y}(nT)]$, etc. This interpretation is made explicit by the following definitions assuming that σ_v is a random variable:

$$\hat{\underline{z}}_0 = E[\underline{z}(0) | p, G_B] \quad (5.4.4)$$

$$\hat{\underline{z}}_n = E[\underline{z}(nT) | p, G_B, \underline{y}(nT)], \quad n \geq 1 \quad (5.4.5)$$

$$\underline{e}_n = \underline{z}(nT) - \hat{\underline{z}}_n, \quad n \geq 0 \quad (5.4.6)$$

$$\underline{P}_0 = p E(\underline{e}_0 \underline{e}_0^T | p, G_B) \quad (5.4.7)$$

$$\underline{P}_n = p E[\underline{e}_n \underline{e}_n^T | p, G_B, \underline{y}(nT)], \quad n \geq 1 \quad (5.4.8)$$

$$\hat{\underline{z}}_0' = E[\underline{z}(T) | p, G_B] \quad (5.4.9)$$

$$\hat{\underline{z}}_n' = E[\underline{z}(nT) | p, G_B, \underline{y}(nT - T)], \quad n \geq 2 \quad (5.4.10)$$

$$\underline{e}_n' = \underline{z}(nT) - \hat{\underline{z}}_n', \quad n \geq 1 \quad (5.4.11)$$

$$P_1^* = pE(\underline{e}_1' \underline{e}_1^T | p, G_B) \quad (5.4.12)$$

$$\underline{P}_n^* = pE[\underline{e}_n' \underline{e}_n^T | p, G_B, \underline{y}(nT - T)], n \geq 2 \quad (5.4.13)$$

In Chapter VII it is shown that \hat{G}_n is a linear combination of the random variables $\underline{y}(nT)$ as before. Based primarily on this result, it can be shown, with the minor alteration of including p in the proofs, that

$$\hat{\underline{z}}_{n+1}' = \underline{\phi}(T) \hat{\underline{z}}_n + (G_B - \hat{G}_n) \underline{\theta}, n \geq 0 \quad (5.4.14)$$

$$\underline{P}_{n+1}^* = \underline{\phi}(T) \underline{P}_n \underline{\phi}^T(T) + \underline{H}, n \geq 0 \quad (5.4.15)$$

where \hat{G}_n is changed as per Chapter VI and \underline{H} is given by

$$\underline{H} = 2b \int_0^T \underline{\phi}(T-x) \underline{B}_2 \underline{B}_2^T \underline{\phi}^T(T-x) dx. \quad (5.4.16)$$

Computation of $\hat{\underline{z}}_0$, $\underline{\theta}_0$, and $\underline{\theta}$ remain unchanged from the previous analysis as, of course, does $e^{\underline{A}t}$. However, the initial covariance matrix \underline{P}_0 is computed from

$$\underline{P}_0 = 2b \int_{-\infty}^0 \underline{\phi}(-t) \underline{B}_2 \underline{B}_2^T \underline{\phi}^T(-t) dt. \quad (5.4.17)$$

Finally, Equations 5.3.9 and 5.3.10 will be retained and Equations 5.3.12 and 5.3.13, for computation of \underline{Q}_n and \underline{q}_n respectively, remain valid.

It should be mentioned that the modifications associated with the assumption that σ_v is a random variable are also discussed in Appendix B.

CHAPTER VI

APPLICATION OF BAYESIAN LEARNING TO SYSTEM

6.1 Definitions and Discussion of Bayesian Learning. This chapter presents a general discussion of the application of Bayesian learning to the system and the "learning equations" are derived first for the case of σ_v known and then for σ_v a random variable.

Several notational definitions are introduced to aid in the succeeding derivations. Define $\underline{y}(n)$ and \underline{y}_n by

$$\underline{y}(n) = \{y(T), \dots, y(nT)\}, \quad n \geq 1 \quad (6.1.1)$$

$$\underline{y}_n = \{y_1, \dots, y_n\}, \quad n \geq 1. \quad (6.1.2)$$

From Equations 5.2.6, 5.2.7, 5.2.11, 5.3.2, and 6.1.2, it follows that

$$\hat{z}_3^1(1) = E[y(T) | G_B] \quad (6.1.3)$$

$$\hat{z}_3^1(n) = E[y(nT) | G_B, \underline{y}(nT - T)], \quad n \geq 2. \quad (6.1.4)$$

Define the sequence $m_{31}(1), m_{32}(1), \dots, m_{31}(n), m_{32}(n), \dots$ by

$$\hat{z}_3^1(n) = m_{31}(n)G_B + m_{32}(n), \quad n \geq 1 \quad (6.1.5)$$

where $m_{31}(n)$ and $m_{32}(n)$ are restricted to not be functions of G_B ; in other words, $m_{31}(n)$ is the coefficient of G_B in $\hat{z}_3^1(n)$ and $m_{32}(n)$ is the remaining term. Define the sequence $p_{33}(1), \dots, p_{33}(n), \dots$ by

$$p_{33}(1) = E\left\{[y(T) - \hat{z}_3^1(1)]^2 | G_B\right\} \quad (6.1.6)$$

$$p_{33}(n) = E\left\{[y(nT) - \hat{z}_3^1(n)]^2 | G_B, \underline{y}(nT - T)\right\}, \quad n \geq 2. \quad (6.1.7)$$

The notation for a normal density function with mean μ and variance

σ^2 will be $N(\mu, \sigma^2)$.

Although the notation used for the sequences might appear overly complicated, it is consistent with that used in Chapter VII. When it is clear from the context, the sampling instant number will be omitted; for example, p_{33} will be used rather than $p_{33}(n)$, \hat{z}_3 rather than $\hat{z}_3^1(n)$, etc.

It was observed in Section 5.3 that the density function $y(nT)$ conditioned by G_B and $y(nT - T)$ is normal; therefore, using the above definitions, one may write

$$f_{y(T)}|G_B \sim N[m_{31}(1)G_B + m_{32}(1), p_{33}(1)] \quad (6.1.8)$$

$$f_{y(nT)}|G_B, y(nT - T) \sim N[m_{31}(n)G_B + m_{32}(n), p_{33}(n)], n \geq 2. \quad (6.1.9)$$

Physically, the sequence of numbers y_1, \dots, y_n, \dots represent the time sequence of measurements of the state z_3 or the difference between velocity error v_e and reference velocity error e_v . The measurements are related to the gyro drift physically by the system or, mathematically, by the state model.

It is desired to find a function \hat{G}_n of the set of measurements which will minimize the expected square of the difference between G_B and \hat{G}_n . That is, one would like to find \hat{G}_n such that $E[(G_B - \hat{G}_n)^2]$ is a minimum. The desired function \hat{G}_n is well known (13) to be given by the equation

$$\hat{G}_n = E[G_B | \underline{y}(n)], n \geq 1. \quad (6.1.10)$$

The estimate \hat{G}_n is used as a control signal to cancel G_B by feeding back $-\hat{G}_n$ to the gyro. Thus Equation 6.1.10 is referred to as the control policy.

To compute \hat{G}_n , it is necessary to know the density function of

G_B conditioned by the measurements $\underline{y}(n)$. The desired density functions will be computed from Bayes' rule; the procedure for estimating a random variable by finding its density function using Bayes' rule and an assumed a priori density function of the random variable is referred to as Bayes' learning.

One might interpret the a priori density as the expression of his previous knowledge of the random variable to be estimated and the density functions given by Equations 6.1.8 and 6.1.9 as an expression of the system behavior. The a posteriori density function he might regard as the blending of system measurements with previous experience. The form of Bayes' rule to be employed is given by

$$f_{G_B|\underline{y}(T)} = \frac{f_{\underline{y}(T)|G_B} f_{G_B}}{f_{\underline{y}(T)}} \quad (6.1.11)$$

$$f_{G_B|\underline{y}(nT)} = \frac{f_{\underline{y}(nT)|G_B, \underline{y}(nT-T)} f_{G_B|\underline{y}(nT-T)}}{f_{\underline{y}(nT)|\underline{y}(nT-T)}}, \quad n \geq 2 \quad (6.1.12)$$

where one will note in Equation 6.1.12 that at each step of applying Bayes' rule, the previous a posteriori density function is used as the a priori density.

6.2 Learning G_B with σ_v Known. In this section it will be assumed that σ_v has the known value of unity. The a priori density function of G_B will be $N(\hat{\mu}_0, \hat{\sigma}_0^2)$ as in Chapter III. Thus

$$f_{G_B} \sim N(\hat{\mu}_0, \hat{\sigma}_0^2). \quad (6.2.1)$$

The desired learning Equations 6.2.3 and 6.2.4 will be given as part of the conclusion of the following theorem.

Theorem 6.2.1. If the density function of G_B is assumed to be given by Equation 6.2.1 and if, for any positive integer n , the conditional density function of $y(nT)$ given $y(nT - T)$ and G_B is assumed to be given by Equation 6.1.8 or 6.1.9, then the density function of G_B , conditioned by $y(nT)$, is of the form

$$f_{G_B|y(nT)} \sim N(\hat{\mu}_n, \hat{\sigma}_n^2) \quad (6.2.2)$$

where $\hat{\sigma}_n$ and $\hat{\mu}_n$ are computed from

$$\hat{\sigma}_n^2 = \frac{p_{33}(n) \hat{\sigma}_{n-1}^2}{p_{33}(n) + \hat{\sigma}_{n-1}^2 m_{31}^2(n)} \quad (6.2.3)$$

$$\hat{\mu}_n = \hat{\sigma}_n^2 \left\{ \frac{\hat{\mu}_{n-1}}{\hat{\sigma}_{n-1}^2} + \frac{m_{31}(n)[y_n - m_{32}(n)]}{p_{33}(n)} \right\}. \quad (6.2.4)$$

This result is identical to that which one would obtain using a Kalman formulation of the problem.

The proof of this theorem is relatively simple since it can be easily established that the a posteriori function is normal by an argument similar to that presented in Section 5.3. Thus the proof can be accomplished by showing Equations 6.2.3 and 6.2.4 are valid.

Nilsson (12) shows that, for normal densities, only the argument of the exponentials of the normal density functions need be considered. He further shows that the normal a posteriori density function is easily established by manipulating the terms of the argument into the form required for the normal density function.

Proof:

Substitution of Equations 6.1.8 and 6.2.1 into Equation 6.1.11 results in

$$f_{G_B|Y(T)}(z|y_1) = J_1 \exp[-(y_1 - m_{31}z - m_{32})^2/2p_{33}] \cdot \exp[-(z - \hat{\mu}_0)^2/2\hat{\sigma}_0^2]$$

where J_1 is a constant. Denoting the argument of the product of the exponentials as \arg_1 , one may proceed

$$\begin{aligned} \arg_1 &= -\frac{(y_1 - m_{31}z - m_{32})^2}{2p_{33}} - \frac{(z - \hat{\mu}_0)^2}{2\hat{\sigma}_0^2} \\ &= -\frac{1}{2} \left\{ (m_{31}^2/p_{33} + 1/\hat{\sigma}_0^2)z^2 - 2[m_{31}(y_1 - m_{32})/p_{33} \right. \\ &\quad \left. + \hat{\mu}_0/\hat{\sigma}_0^2]z + \hat{\mu}_0^2/\hat{\sigma}_0^2 + m_{32}^2/p_{33} \right\}. \end{aligned}$$

Setting $n = 1$ in Equations 6.2.3 and 6.2.4 and substituting into the expression for \arg_1 gives, after completing the square in z ,

$$\arg_1 = -\frac{(z - \hat{\mu}_1)^2}{2\hat{\sigma}_1^2} - \frac{m_{32}^2}{2p_{33}} - \frac{\hat{\mu}_0^2}{2\hat{\sigma}_0^2} + \frac{\hat{\mu}_1^2}{2\hat{\sigma}_1^2}.$$

Thus the a posteriori density function has the desired form as one can see by identifying the first term as the argument of the exponential.

To complete the proof, one can show, in a manner exactly similar to that above, if the form of the a priori density given by Equation 6.2.2 for $n = 1$ and Equation 6.1.9 are substituted into Equation 6.1.12, then using Equations 6.2.3 and 6.2.4 will result in the a posteriori density function being given by Equation 6.2.2. Therefore, by induction, the theorem is proved.

6.3 Learning G_B with σ_v Unknown. In the previous section, where σ_v was known, the assumption that G_B was a normal random variable resulted in the a priori and a posteriori density functions being of the same type; specifically, they were both normal. This so called repro-

ducing property is quite desirable (8) from a computational point of view. Both $p(\sigma_v^{-2})$ and G_B are assumed to be random variables in this section and, in order to obtain the reproducing property, the a priori density function will have to be modified.

In keeping with the discussion of Section 5.4, Equations 6.1.6 and 6.1.7 will have to be altered to reflect Equations 5.4.9 through 5.4.12 as follows:

$$p_{33}(1) = p \ E\{[y(T) - \hat{z}_3^1(1)]^2 | p, G_B\} \quad (6.3.1)$$

$$p_{33}(n) = p \ E\{[y(nT) - \hat{z}_3^1(n)]^2 | p, G_B, y(nT - T)\}, \ n \geq 2. \quad (6.3.2)$$

Therefore the density function of $y(nT)$, conditioned by p , G_B , and the previous measurements, is given by

$$f_{y(T)} | p, G_B \sim N[m_{31}(1)G_B + m_{32}(1), p_{33}(1)/p] \quad (6.3.3)$$

$$f_{y(nT)} | p, G_B, y(nT - T) \sim N[m_{32}(n)G_B + m_{32}(n), p_{33}(n)/p], \ n \geq 2. \quad (6.3.4)$$

Keehn (8) shows that if a normal inverted-Wishart joint density function is used as the a priori density for Bayesian learning of independent patterns with unknown means and covariances, then the reproducing property is obtained. Motivated by his results, one can define the joint a priori density function for G_B and p to follow a normal inverted-Wishart law; that is, for $u > 0$, $r_0 > 3$,

$$f_{G_B, p}(z, u) = \left\{ \left(\frac{w_0 u}{2\pi} \right)^{1/2} \exp[-w_0 u (z - \hat{\mu}_0)^2 / 2] \right\} \cdot \left\{ \left(\frac{r_0 s_0}{2} \right)^{\frac{r_0 - 1}{2}} \frac{u^{\frac{r_0 - 3}{2}}}{\Gamma\left(\frac{r_0 - 1}{2}\right)} \exp(-r_0 s_0 u / 2) U(u) \right\} \quad (6.3.5)$$

where $\Gamma(\cdot)$ is the gamma function and $U(\cdot)$ is the unit step function. Examination of Equation 6.3.5 reveals that G_B is distributed normally with mean $\hat{\mu}_0$ and variance $1/w_0 u$ where w_0 reflects the confidence one has that $\hat{\mu}_0$ is the true mean. The variance follows an inverted-Wishart law with parameters r_0 and s_0 .

The symbol W_i will be used to denote a joint normal, inverted-Wishart probability density function with parameters $\hat{\mu}_i$, w_i , r_i and s_i ; thus

$$f_{G_B, p}(z, u) \sim W_0.$$

Also \tilde{K}_i will be defined by

$$\tilde{K}_i = \frac{\left(\frac{w_i}{2\pi}\right)^{1/2} \left(\frac{r_i s_i}{2}\right)^{\frac{r_i-1}{2}}}{\Gamma\left(\frac{r_i-1}{2}\right)}. \quad (6.3.6)$$

Therefore

$$W_i = \tilde{K}_i u^{(r_i-2)/2} \exp[-w_i (z - \hat{\mu}_i)^2 u/2 - r_i s_i u/2] U(u). \quad (6.3.7)$$

It will now be shown that the following choice of recursive relations results in the reproducing property for the learning procedure:

$$w_i = w_{i-1} + m_{31}^2(i)/p_{33}(i) \quad (6.3.8)$$

$$w_i \hat{\mu}_i = \hat{\mu}_{i-1} w_{i-1} + m_{31}(i)[y_i - m_{32}(i)]/p_{33}(i) \quad (6.3.9)$$

$$r_i = r_{i-1} + 1 \quad (6.3.10)$$

$$r_i s_i = r_{i-1} s_{i-1} + [y_i - m_{32}(i)]^2 / p_{33}(i) + \hat{\mu}_{i-1}^2 w_{i-1} - \hat{\mu}_i^2 w_i. \quad (6.3.11)$$

Rather than rewrite Equations 6.1.8, 6.1.9, 6.1.11, and 6.1.12 to reflect the additional random variable p , it will be noted that ob-

vious changes in notation must be made.

Using Equations 6.3.5 and 6.3.3, one can write

$$f(y_1|z,u)f(z,u) = (u/2\pi p_{33})^{1/2} \exp[-u(y_1 - m_{31}z - m_{32})^2/2p_{33}] \cdot \\ \tilde{K}_0 u^{\frac{r_0-2}{2}} \exp[-w_0(z - \hat{\mu}_0)^2 u/2 - r_0 s_0/2] U(u). \quad (6.3.12)$$

Combining the products of exponentials into the exponential of the sum, completing the square in z , and substitution of Equations 6.3.8 through 6.3.11 gives

$$f(y_1|z,u)f(z,u) = \frac{\tilde{K}_0 u^{\frac{r_1-2}{2}}}{\sqrt{2\pi p_{33}}} \exp[-w_1(z - \hat{\mu}_1)^2 u/2 - r_1 s_1 u/2] U(u). \quad (6.3.13)$$

Using Equation 6.3.7, one can rewrite Equation 6.3.13 as

$$f(y_1|z,u)f(z,u) \sim \tilde{K}_0 W_1 / \tilde{K}_1 \sqrt{2\pi p_{33}}. \quad (6.3.14)$$

Now $f(y_1)$ can be evaluated from Equation 6.3.14 as follows:

$$f(y_1) = \int_{-\infty}^{\infty} \int_{-\infty}^{\infty} f(y_1|z,u)f(z,u) dz du \\ = \frac{\tilde{K}_0}{\tilde{K}_1 \sqrt{2\pi p_{33}}} \int_{-\infty}^{\infty} \int_{-\infty}^{\infty} W_1 dz du \\ = \frac{\tilde{K}_0}{\tilde{K}_1 \sqrt{2\pi p_{33}}}. \quad (6.3.15)$$

Substitution of Equations 6.3.14 and 6.3.15 into Equation 6.1.11 yields

$$f(z,u|y_1) \sim W_1. \quad (6.3.16)$$

Thus, at the first step of the computational sequence, the reproducing

property is exhibited.

Similarly, using

$$f(z, u | \underline{y}_n) \sim W_n,$$

Equations 6.3.8 through 6.3.11, Equation 6.3.4, and Bayes' rule, one can show

$$f(z, u | \underline{y}_{n+1}) \sim W_{n+1}. \quad (6.3.18)$$

Therefore, by induction, the following theorem is proved:

Theorem 6.3.1. If the a priori density function given by Equation 6.3.1 is used in Bayes' rule, Equations 6.1.11, and Equation 6.1.12, and if Equations 6.3.8 through 6.3.11 are employed recursively, then, for each $i = 1, 2, \dots$, the a posteriori density function is given by Equation 6.3.7

Equations 6.3.8 and 6.3.9 will be referred to as the learning equations for σ_v unknown. Finally, by direct integration, one can obtain the control policy

$$\hat{G}_n = \hat{\mu}_n, \quad n \geq 1. \quad (6.3.19)$$

Thus \hat{G}_n is a linear combination of the a priori mean $\hat{\mu}_0$ and the set of measurements $\underline{y}(n)$

$$\hat{G}_n = \left\{ \hat{\mu}_0 w_0 + \sum_{k=1}^n m_{31}(k) [y(kT) - m_{32}(k)] / p_{33}(k) \right\} / w_n.$$

CHAPTER VII

ALGORITHMS FOR COMPUTING \hat{G}_n

7.1 Computational Procedure for Evaluating \hat{G}_n when σ_v is Known.

In this section the recursive solution for estimating G_B is obtained under the assumption that the value of σ_v is known. It was found expedient to define two sets of 3×2 matrices \underline{M}_n and \underline{Z}_n by the following equations:

$$\hat{\underline{Z}}'_n = \underline{M}_n \begin{bmatrix} G_B \\ 1 \end{bmatrix} \quad (7.1.1)$$

$$\hat{\underline{Z}}_n = \underline{Z}_n \begin{bmatrix} G_B \\ 1 \end{bmatrix} \quad (7.1.2)$$

where $\underline{M}_n = [m_{ij}(n)]$ and $\underline{Z}_n = [z_{ij}(n)]$. The elements $m_{ij}(n)$ and $z_{ij}(n)$ are restricted so as not to contain G_B . Thus the first columns of the matrices, denoted \underline{M}_n^1 and \underline{Z}_n^1 respectively, are the vectors of coefficients of G_B while the second columns, denoted respectively \underline{M}_n^2 and \underline{Z}_n^2 , are vectors of the remaining terms.

From Property B.4.5 and Equations A.12 and 7.1.1, one may proceed

$$\begin{aligned} \hat{\underline{Z}}'_1 &= \underline{\phi}(T) \hat{\underline{Z}}'_0 + (G_B - \hat{G}_0) \underline{\theta} \\ &= \begin{bmatrix} \phi_{11}(T) & \phi_{12}(T) & \phi_{13}(T) \\ \phi_{21}(T) & \phi_{22}(T) & \phi_{23}(T) \\ \phi_{31}(T) & \phi_{32}(T) & \phi_{33}(T) \end{bmatrix} \begin{bmatrix} -1 \\ K_1/g \\ -1 \end{bmatrix} \frac{R}{1 + K_2} G_B + \begin{bmatrix} \theta_1 \\ \theta_2 \\ \theta_3 \end{bmatrix} (G_B - \hat{G}_0) \end{aligned}$$

$$\hat{\underline{z}}_1' = \underline{M}_1 \begin{bmatrix} G_B \\ 1 \end{bmatrix} \quad (7.1.3)$$

where, for $i = 1, 2, 3$

$$\begin{aligned} m_{i1}(1) &= [-\theta_{i1}(T) + K_2 \theta_{i2}(T)/g - \theta_{i3}(T)] R / (1 + K_2) + \theta_{i1} \\ m_{i2}(1) &= \theta_{i1} \hat{G}_0. \end{aligned} \quad (7.1.4)$$

The associated covariance matrix \underline{P}_1^* can be computed by substitution of \underline{P}_0 , given by Equation 5.2.4, into the equation of Property B.4.6.

Using the learning Equations 6.2.3 and 6.2.4 along with Equation 6.1.10 one can obtain the first control \hat{G}_1 as follows:

$$\hat{\sigma}_1^2 = \hat{\sigma}_0^2 p_{33}(1) / [p_{33}(1) + \hat{\sigma}_0^2 m_{31}^2(1)] \quad (7.1.5)$$

$$\hat{\mu}_1 = \hat{\sigma}_1^2 \hat{\mu}_0 / \hat{\sigma}_0^2 + \hat{\sigma}_1^2 m_{31}(1) [y_1 - m_{32}(1)] / p_{33}(1) \quad (7.1.6)$$

$$\hat{G}_1 = \hat{\mu}_1. \quad (7.1.7)$$

Computation of $\hat{\underline{z}}_1$ and \underline{P}_1 can be performed using Equations 5.3.3, 5.3.13, 5.3.12, and 5.3.5 in the following manner:

$$\hat{\underline{z}}_1 = \begin{bmatrix} \hat{z}_1' + p_{13}(y_1 - \hat{z}_3')/p_{33} \\ \hat{z}_2' + p_{23}(y_1 - \hat{z}_3')/p_{33} \\ y_1 \end{bmatrix} \quad (7.1.8)$$

$$\underline{Q}_1 = \begin{bmatrix} p_{11} - p_{13}^2/p_{33} & p_{12} - p_{13}p_{23}/p_{33} \\ p_{21} - p_{13}p_{23}/p_{33} & p_{22} - p_{23}^2/p_{33} \end{bmatrix} \quad (7.1.9)$$

$$\underline{P}_1 = \begin{bmatrix} \underline{Q}_1 & \underline{0} \\ \underline{0}^T & 0 \end{bmatrix}. \quad (7.1.10)$$

Equation 7.1.8 can be put into the form of Equation 7.1.2 using Equation 7.1.3 as follows:

$$\begin{aligned} \hat{\underline{z}}_i &= \begin{bmatrix} m_{11}G_B + m_{12} + p_{13}(y_i - m_{31}G_B - m_{32})/p_{33} \\ m_{21}G_B + m_{22} + p_{23}(y_i - m_{31}G_B - m_{32})/p_{33} \\ y_i \end{bmatrix} \\ &= \underline{z}_1^1 G_B + \underline{z}_1^2 \end{aligned} \quad (7.1.11)$$

where, for $i = 1, 2$,

$$z_{i1} = m_{i1} - p_{i3}m_{31}/p_{33} \quad (7.1.12)$$

$$z_{i2} = m_{i2} + p_{i3}(y_1 - m_{32})/p_{33} \quad (7.1.13)$$

and

$$z_{31} = 0 \quad (7.1.14)$$

$$z_{32} = y_1. \quad (7.1.15)$$

The above computations form a complete set for the first sampling estimate. For the n^{th} sampling instant, one assumes that \hat{G}_{n-1} ,

$$\hat{\underline{z}}_{n-1} = \underline{z}_{n-1} \begin{bmatrix} G_B \\ 1 \end{bmatrix} \quad (7.1.16)$$

and

$$\underline{P}_{n-1} = \begin{bmatrix} \underline{Q}_{n-1} & \underline{0} \\ \underline{0}^T & 0 \end{bmatrix} \quad (7.1.17)$$

have been computed. Then he may compute \underline{P}_n^* from

$$\underline{P}_n^* = \underline{\phi}(T) \underline{P}_{n-1} \underline{\phi}^T(T) + \underline{H} \quad (7.1.18)$$

and $\hat{\underline{z}}_n'$ as follows:

$$\hat{\underline{z}}_n' = \underline{\phi}(T) \hat{\underline{z}}_{n-1} + (G_B - \hat{G}_{n-1}) \underline{\theta}$$

$$\begin{aligned}
\hat{z}_n^1 &= \underline{\varnothing}(T) (\underline{z}_{n-1}^1 G_B + \underline{z}_{n-1}^2) + (G_B - \hat{G}_{n-1}) \underline{\vartheta} \\
&= [\underline{\varnothing}(T) \underline{z}_{n-1}^1 + \underline{\vartheta}] G_B + [\underline{\varnothing}(T) \underline{z}_{n-1}^2 - \underline{\vartheta} \hat{G}_{n-1}]. \quad (7.1.19)
\end{aligned}$$

Thus

$$\underline{M}_n^1 = \underline{\varnothing}(T) \underline{z}_{n-1}^1 + \underline{\vartheta} \quad (7.1.20)$$

$$\underline{M}_n^2 = \underline{\varnothing}(T) \underline{z}_{n-1}^2 - \underline{\vartheta} \hat{G}_{n-1}. \quad (7.1.21)$$

At this stage in the computations, the control \hat{G}_n can be computed using Equations 7.1.18, 7.1.20, and 7.1.21 in the following equations:

$$\hat{\sigma}_n^2 = p_{33}(n) \hat{\sigma}_{n-1}^2 / [p_{33}(n) + \hat{\sigma}_{n-1}^2 m_{31}^2(n)] \quad (7.1.22)$$

$$\hat{\mu}_n = \frac{\hat{\sigma}_n^2 \hat{\mu}_{n-1}}{\hat{\sigma}_{n-1}^2} + \frac{\hat{\sigma}_n^2 m_{31}(n) [y_n - m_{32}(n)]}{p_{33}(n)} \quad (7.1.23)$$

$$\hat{G}_n = \hat{\mu}_n. \quad (7.1.24)$$

To complete the computations for the n^{th} sampling instant, the \underline{z}_n matrix can be obtained from

$$z_{i1}(n) = m_{i1}(n) - p_{i3}(n) m_{32}(n) / p_{33}(n), \quad i = 1, 2 \quad (7.1.25)$$

$$z_{i2}(n) = m_{i2}(n) - p_{i3}(n) [y_n - m_{32}(n)] / p_{33}(n), \quad i = 1, 2 \quad (7.1.26)$$

$$z_{31}(n) = 0 \quad (7.1.27)$$

$$z_{32}(n) = y_n \quad (7.1.28)$$

and \underline{P}_n can be found using Equations 5.3.12 and 7.1.17.

7.2 Computational Procedure for Evaluating \hat{G}_n when σ_v is Unknown. The previous section presented a detailed computational proce-

ture under the assumption that σ_v is known. When the assumption is made that σ_v is a random variable, all of the above procedure remains unchanged with the following exceptions:

Exception a. Equation 7.1.5 is replaced by

$$w_1 = w_0 + m_{31}(1)/p_{33}(1) \quad (7.2.1)$$

and Equation 7.1.6 is replaced by

$$\hat{\mu}_1 = \frac{\hat{\mu}_0 w_0 + m_{31}(1)[y_1 - m_{32}(1)]/p_{33}(1)}{w_1} \quad (7.2.2)$$

Exception b. Equation 7.1.22 is replaced by

$$w_n = w_{n-1} + m_{31}^2(n)/p_{33}(n) \quad (7.2.3)$$

and Equation 7.1.23 is replaced by

$$\hat{\mu}_n = \frac{\hat{\mu}_{n-1} w_{n-1} + m_{31}(n)[y_n - m_{32}(n)]/p_{33}(n)}{w_n} \quad (7.2.4)$$

The matrices \underline{H} and \underline{P}_0 do not have to be changed since they were computed for a unity value of σ_v . If, however, it had been assumed that σ_v was some other known value in the previous section, \underline{H} and \underline{P}_0 would have to be recomputed for the assumption σ_v is a random variable.

7.3 Summary. In this chapter the recursive estimate \hat{G}_n for G_B was obtained both for σ_v known and unknown; the recursive relationships for these two cases were shown to be nearly identical. The computational sequence was started with \hat{z}_0 and \underline{P}_0 ; then the matrices \underline{M}_n , \underline{Z}_n , \underline{P}_n and \underline{P}_n^* were computed recursively with the parameters $\hat{\sigma}_n$, $\hat{\mu}_n$, and \hat{G}_n being computed at each step. Although the computations required

become very tedious for hand calculation, their recursive nature is ideally suited to digital computer evaluation.

CHAPTER VIII

EMPIRICAL LEARNING

8.1 Introduction. In this chapter the assumptions that G_B is a normal random variable and that $v(t)$ is a normal random process will be relaxed. It is therefore assumed that a time sequence of measurements $y(kT)$ are available of the state $z_3(t)$ from which an estimate \hat{G}_n of G_B is to be constructed. As before, the estimate \hat{G}_n will be applied as a control signal to cancel the unwanted gyro drift G_B .

The author has arbitrarily selected the term empirical learning to describe the estimation procedure used although some other terminology would serve equally as well. The choice resulted from investigations of the empirical distribution function (15).

8.2 Empirical Estimate. The assumptions made in this chapter will now be reviewed. The state model presented in Chapter III and illustrated in Figure 3.4.2 will be used. The gyro drift G_B is assumed to be a random variable and the driver $v(t)$ is assumed to be a white stationary random process with zero mean and autocorrelation function

$$E[v(t)v(t + \tau)] = \delta(\tau). \quad (8.2.1)$$

The variance σ_v^2 of the reference velocity error $e_v(t)$ is assumed to be a fixed unknown number. The other system parameters are assumed unchanged.

As before, it is assumed that the first measurement $y(T)$ is

available at time T and the other measurements are made at equal time intervals. It is desired to form a new estimate \hat{G}_n of G_B as each measurement is observed.

The recursive solution to the state equation was shown in Chapter IV to be

$$\underline{z}(T) = \underline{\theta}_0 G_B + \underline{g}_1 \quad (8.2.2)$$

$$\underline{z}(nT) = \underline{\phi}(T) \underline{z}(nT - T) + (G_B - \hat{G}_{n-1}) \underline{\theta} + \underline{g}_n, \quad n \geq 2 \quad (8.2.3)$$

$$y(nT) = \underline{C} \underline{z}(nT) \quad (8.2.4)$$

where the notation used in Equation 8.2.2 has been altered slightly to account for the fact that no control is applied over the time interval from zero to the first sampling instant.

The solution, in nonrecursive form, can be written

$$\begin{aligned} \underline{z}(nT) = & \underline{\theta}_0 G_B + \sigma_v \sqrt{2b} \int_{-\infty}^{nT} \underline{\phi}(nT - t) \underline{B}_2 v(t) dt \\ & - \sum_{k=1}^n \underline{\phi}^{n-k}(T) \underline{\theta} \hat{G}_{k-1}, \quad n \geq 1 \end{aligned} \quad (8.2.5)$$

where $\hat{G}_0 = 0$. Letting

$$\underline{s}_1 = \underline{0}$$

$$\underline{s}_n = \underline{\theta} \hat{G}_{n-1} + \underline{\phi}(T) \underline{s}_{n-1}, \quad n \geq 2 \quad (8.2.6)$$

$$\underline{G}(n) = \underline{z}(nT) + \underline{s}_n, \quad n \geq 1 \quad (8.2.7)$$

gives

$$\underline{G}(n) = \underline{\theta}_0 G_B + \sigma_v \sqrt{2b} \int_{-\infty}^{nT} \underline{\phi}(nT - t) \underline{B}_2 v(t) dt. \quad (8.2.8)$$

Summing the terms of Equation 8.2.8 gives

$$\sum_{k=1}^n \underline{G}(k) = n \underline{\theta}_0 G_B + \sigma_v \sqrt{2b} \sum_{k=1}^n \underline{\phi}(kT - t) \underline{B}_2 v(t) dt. \quad (8.2.9)$$

The empirical estimate \hat{G}_n will be defined by

$$\hat{G}_n = \frac{1}{n \theta_{03}} \sum_{k=1}^n \underline{C} \underline{G}(k) \quad (8.2.10)$$

where θ_{03} is the third element of the vector $\underline{\theta}_0$. Thus

$$\hat{G}_n = G_B + \frac{K}{n} \sum_{k=1}^n \int_{-\infty}^{kT} \phi_{33}(kT - t) v(t) dt \quad (8.2.11)$$

where $K = \sigma_v \sqrt{2b} / \theta_{03}$. Taking the expected value of Equation 8.2.11 gives

$$E(\hat{G}_n | G_B) = G_B. \quad (8.2.12)$$

Hence \hat{G}_n is an unbiased estimate of G_B .

The variance $\sigma_{\text{emp}}^2(n)$ of \hat{G}_n about G_B is given by

$$\sigma_{\text{emp}}^2(n) = E[(\hat{G}_n - G_B)^2]. \quad (8.2.13)$$

To express this variance, the following preliminary computation is made:

$$\beta(n) = E\left[\frac{K^2}{n^2} \sum_{k=1}^n \int_{-\infty}^{kT} \underline{\phi}(kT - t) \underline{B}_2 v(t) dt\right]$$

$$\sum_{m=1}^n \int_{-\infty}^{mT} \underline{B}_2^T \underline{\phi}^T(mT - x) v(x) dx]$$

$$= \frac{K^2}{n^2} \sum_{k=1}^n \sum_{m=1}^n \int_{-\infty}^{kT} \int_{-\infty}^{mT}$$

$$\underline{\phi}(kT - t) \underline{B}_2 \underline{B}_2^T \underline{\phi}^T(mT - x) E[v(t) v(x)] dx dt$$

$$\begin{aligned}
\beta(n) &= \frac{K^2}{n^2} \sum_{k=1}^n \left\{ \sum_{m=1}^k \int_{-\infty}^{mT} \phi(kT - t) \underline{B}_2 \underline{B}_2^T \phi(mT - t) dt \right. \\
&\quad \left. + \sum_{m=k+1}^n \int_{-\infty}^{kT} \phi(kT - t) \underline{B}_2 \underline{B}_2^T \phi(mT - t) dt \right\} \\
&= \frac{K^2}{n^2} \sum_{k=1}^n \left\{ \sum_{m=1}^k \phi(kT - mT) \underline{P}_0 + \underline{P}_0 \sum_{m=k+1}^n \phi^T(mT - kT) \right\}. \quad (8.2.14)
\end{aligned}$$

Using Equation 8.2.10, one can rewrite Equation 8.2.13 as

$$\sigma_{\text{emp}}^2(n) = E \left\{ \sum_{k=1}^n \underline{C} [\underline{G}(k) - \underline{\Theta}_0 \underline{G}_B] \sum_{m=1}^n [\underline{G}(m) - \underline{\Theta}_0 \underline{G}_B]^T \underline{C}^T \right\}. \quad (8.2.15)$$

Combining Equations 8.2.14 and 8.2.15 as per Equation 8.2.9 results in the following expression for the variance:

$$\begin{aligned}
\sigma_{\text{emp}}^2(n) &= \frac{K^2}{n^2} \sum_{k=1}^n \left\{ \sum_{m=1}^k \underline{C} \phi(kT - mT) \underline{P}_0 \right. \\
&\quad \left. + \underline{P}_0 \sum_{m=k+1}^n \phi^T(mT - kT) \underline{C}^T \right\}. \quad (8.2.16)
\end{aligned}$$

If one uses the constituent matrix representation of the transition matrices, he can show, by elementary series methods, that the right hand side of Equation 8.2.16 tends to zero as n increases without bound. The details of this cumbersome but straightforward computation will not be included in this thesis. One has the result that

$$\lim_{n \rightarrow \infty} \sigma_{\text{emp}}^2(n) = 0. \quad (8.2.17)$$

8.3 Recursive Empirical Estimate. It is desirable to express the empirical estimate recursively as was done for the Bayes' formulation. This can be done by combining Equations 8.2.6, 8.2.7, and

8.2.10 into the following form:

$$\hat{G}_n = \sum_{k=1}^n [y(kT) + \underline{C} \underline{S}_k] / n\theta_{03}, \quad n \geq 1. \quad (8.3.1)$$

Then the recursive estimate will be

$$\hat{G}_{n+1} = \frac{n\hat{G}_n}{n+1} + [y(nT + T) + \underline{C} \underline{S}_{n+1}] / \theta_{03}^{(n+1)}, \quad n \geq 1. \quad (8.3.2)$$

Thus to form the empirical estimate \hat{G}_n it is necessary to store the previous estimate and the vector \underline{S}_{n-1} ; then, as the new measurement is obtained, the old estimate is updated by Equation 8.3.2 to reflect the additional information. The reader can observe that the terms of Equation 8.3.1 which involve $y(kT)$ represent the sample mean of the measurements multiplied by the inverse transition parameter θ_{03}^{-1} while those terms involving \underline{S}_k represent the compensation for the control signal sequence.

By making the following definitions, the empirical variance can also be cast into a recursive form:

$$\underline{P}_e(n) = \frac{K^2}{n^2} \sum_{k=1}^n \left\{ \sum_{m=1}^k \underline{\theta}(kT-mT) \underline{P}_0 + \underline{P}_0 \sum_{m=k+1}^n \underline{\theta}(mT-kT) \right\}, \quad n \geq 1 \quad (8.3.3)$$

$$\underline{\alpha}(n) = K^2 \sum_{j=1}^n [\underline{\theta}(jT-T) \underline{P}_0 + \underline{P}_0 \underline{\theta}^T(jT-T)], \quad n \geq 1. \quad (8.3.4)$$

Equation 8.3.4 can immediately be put into the recursive form

$$\underline{\alpha}(n+1) = \underline{\alpha}(n) + K^2 [\underline{\theta}(nT) \underline{P}_0 + \underline{P}_0 \underline{\theta}^T(nT)], \quad n \geq 2. \quad (8.3.5)$$

Using Equations 8.3.3 and 8.3.5, one can also show

$$\underline{P}_e(n+1) = \frac{n^2 \underline{P}_e(n) + \underline{\alpha}(n+1)}{(n+1)^2}, \quad n \geq 2. \quad (8.3.6)$$

Then the empirical variance is given by

$$\sigma_{\text{emp}}^2(n) = \underline{C} \underline{P}_e(n) \underline{C}^T, \quad n \geq 1. \quad (8.3.7)$$

Therefore the desired recursive form of the variance is given by Equations 8.3.5 through 8.3.7.

CHAPTER IX

DISCUSSION AND COMPARISON OF ESTIMATION METHODS

9.1 Introduction. In this chapter characteristics of the various methods of estimating gyro drift are considered and some comparisons between them are made. To generate data for the recursive estimate, digital computer simulation and computation were employed. The computer simulation can be grouped into two classes: those runs for which reference velocity noise was simulated and those without noise simulated. The former group served the primary purpose of verifying the theoretical performance predictions while the latter provided data for comparison of the estimation methods.

The computer runs without noise simulated can be considered to represent the expected estimate of the gyro drift conditioned by the gyro drift value. Thus the normalized curves of \hat{G}_n/G_B may be interpreted as the ensemble average of a large number of sample functions.

9.2 Estimating G_B with Known Variance. Illustrated in Figures 9.2.1 through 9.2.4 are the characteristics of the Bayesian learning procedure for a known velocity error variance of one foot²/second². As illustrated in Figures 9.2.1 and 9.2.2, decreasing the time between samples tends to improve the speed of convergence. However, as one might suspect from the fact that there is a pole at minus one, decreasing the sampling time below one second does not greatly increase the convergence speed as can be seen from Figure 9.2.1. Intui-

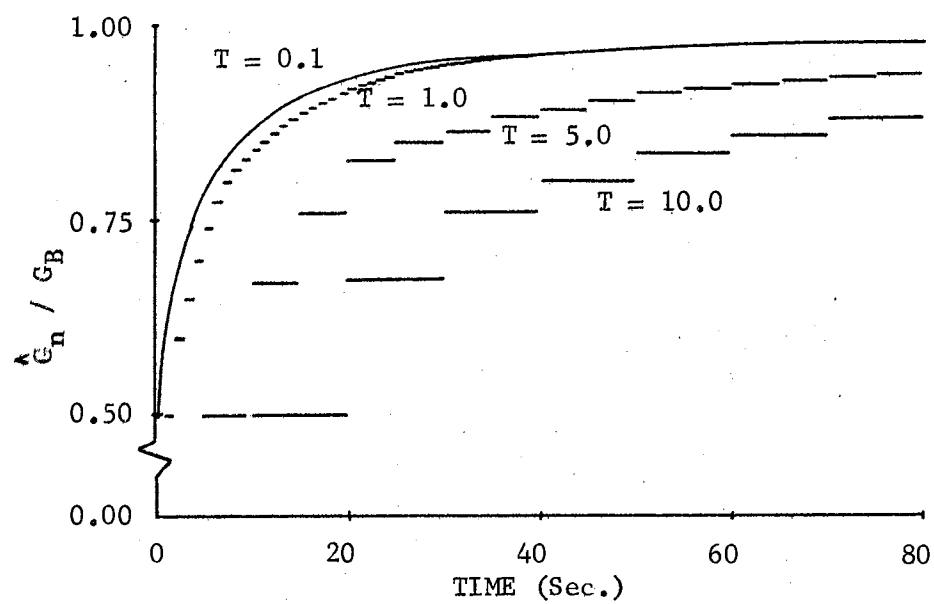


Figure 9.2.1. Effect of Changing Sample Time on G_n^A

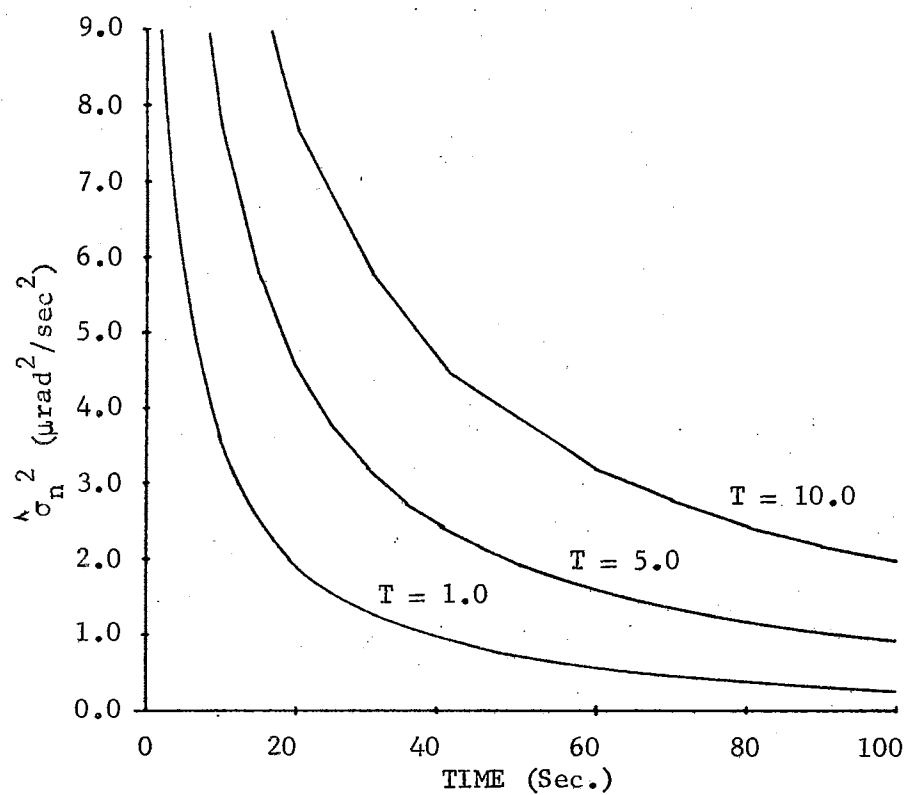


Figure 9.2.2. Effect of Changing Sample Time on $\sigma_n^A^2$

tively one would expect a larger sampling rate to speed convergence since information is available at a faster rate which is confirmed by the curves. The data illustrated are for the nominal values of zero and one degree per hour for $\hat{\mu}_0$ and $\hat{\sigma}_0$ respectively.

The effect of varying the a priori density parameters $\hat{\mu}_0$ and $\hat{\sigma}_0$ for a sampling period of one second is illustrated in Figures 9.2.3 and 9.2.4 respectively where smoothed curves are drawn through the data points. Varying the a priori mean has the effect which one would expect including symmetry about G_B . Small values of $\hat{\sigma}_0$ imply that one has confidence in the a priori mean and correspondingly less confidence in the measurements; this is borne out in the slower convergence speed observed in the curves for the smaller a priori variance values.

Figure 9.2.5 presents a comparison between the variance of the estimate (about the true value of gyro drift) for the empirical method and the known variance Bayesian learning technique; while the sampling period for these curves is one second, the curves for other sampling periods are similar. Using a mean squared-error criteria, the curves clearly indicate that one would prefer the Bayesian approach for cases with specified noise variances.

It is interesting to compare the convergence rates of the Bayesian and empirical estimates with the time response of the third-order leveling system as shown in Figure D.2. The normalized mean value of the empirical estimate is unity since it is an unbiased estimate; one may examine the mean squared error as a function of time, Figure 9.2.5, as a measure of convergence speed. The speeds of response for the recursive estimation methods are much faster than that for the third-order system.

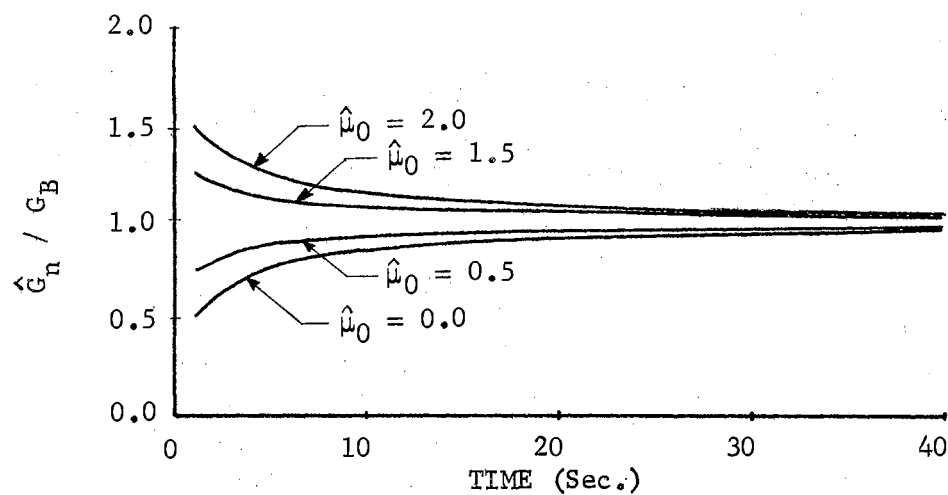


Figure 9.2.3. Effect of Changing $\hat{\mu}_0$

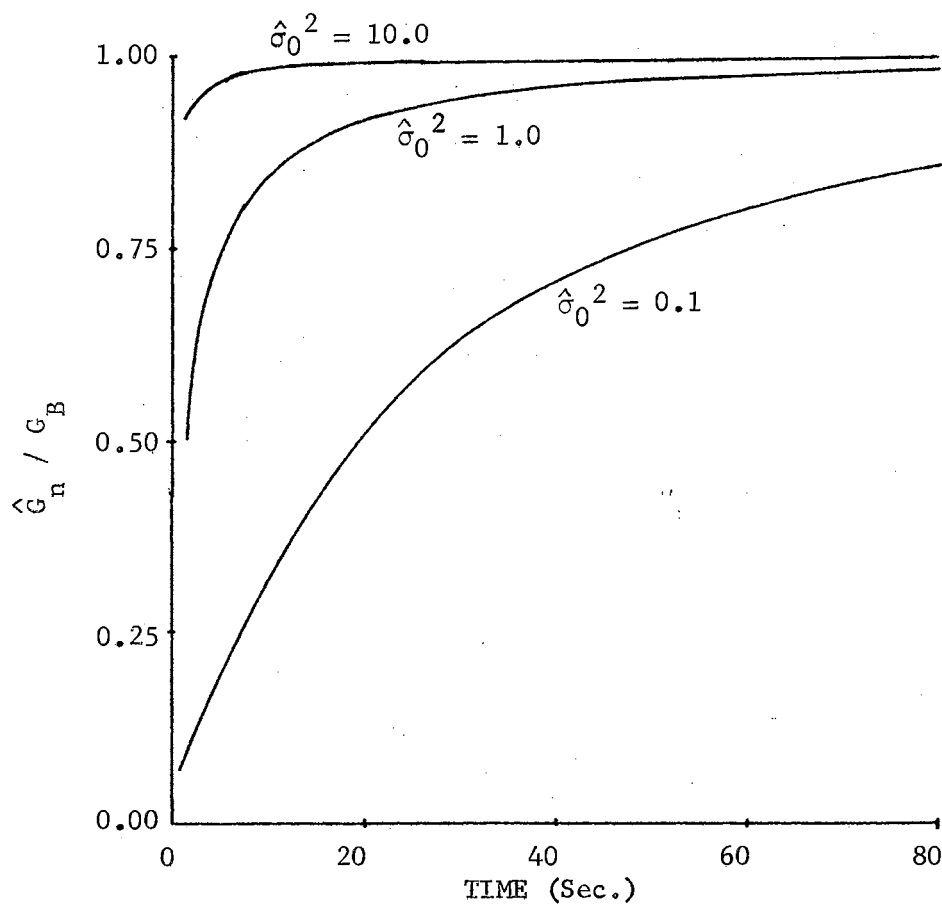


Figure 9.2.4. Effect of Changing $\hat{\sigma}_0$

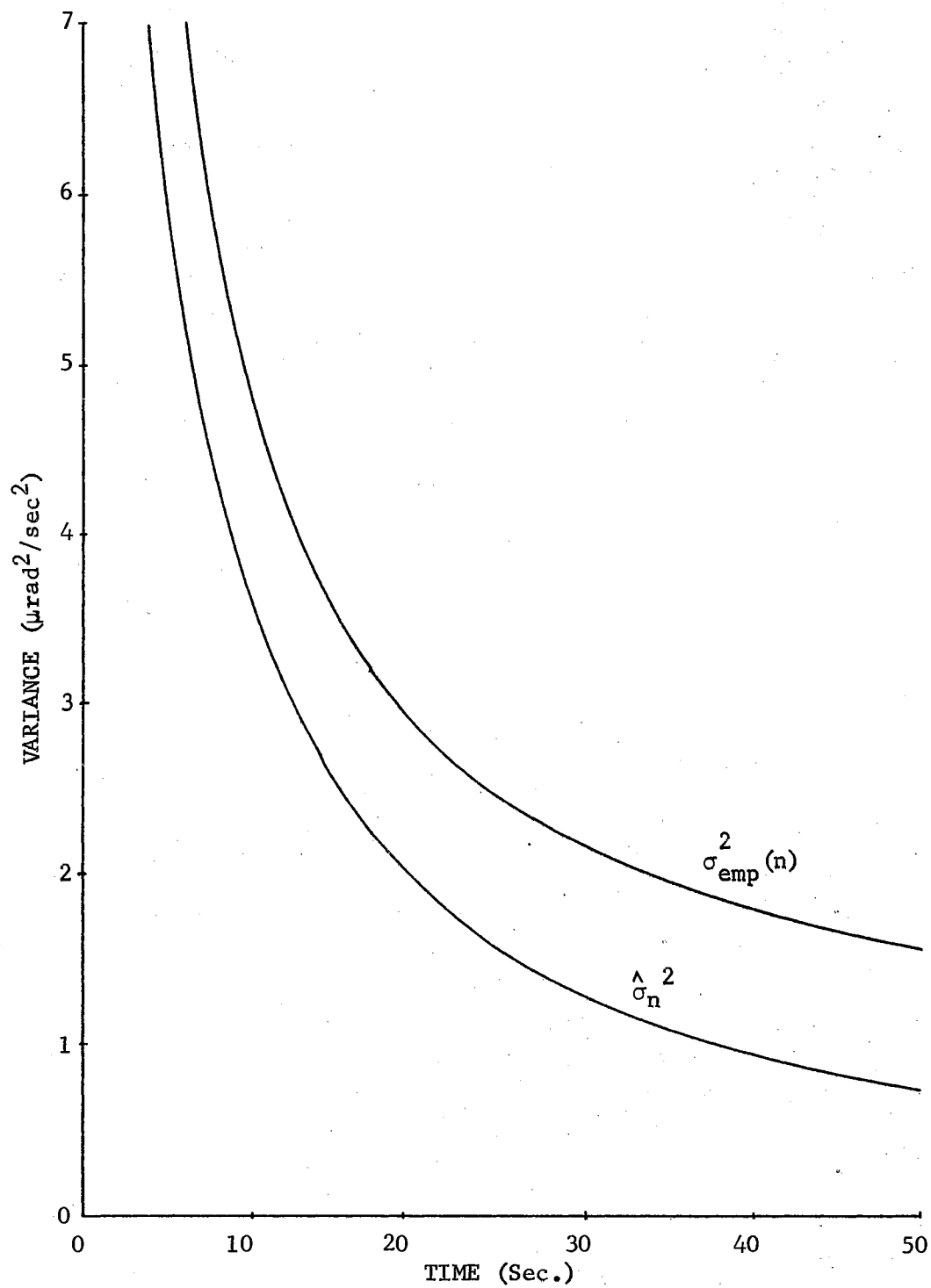


Figure 9.2.5. Comparison of Bayes (with Known Noise) Variance to Empirical Variance

9.3 Estimating G_B with Unknown Variance. Use of the Gaussian-inverted Wishart density provides a means whereby one can find a recursive Bayesian estimate of the mean if the variance is unknown. From an engineering point of view, the formulation appears most desirable for in many applications the variance is not known.

However, if one compares the Bayesian learning equations for the case of known variance, Equations 6.2.3 and 6.2.4, with those for unspecified variance, Equations 6.3.8 and 6.3.9, he finds them to be identical by letting

$$\hat{\sigma}_k^2 = 1/w_k. \quad (9.3.1)$$

In formulating the sets of recursive conditional expectations, the two cases differed in that a random variable p was introduced for σ_v^{-2} when the variance was unknown. Essentially this is equivalent to normalizing the unknown variance; that is, if the true value of σ_v is unknown, the Gaussian-inverted Wishart formulation is identical to the known variance formulation with the value of σ_v taken as unity.

Since, in the case for known variance σ_v was actually unity, the curves presented in Figures 9.2.1 through 9.2.4 also represent the behavior of the unknown variance case if Equation 9.3.1 is employed.

In reference to Equation 6.3.5, the Gaussian-inverted Wishart a posteriori density function was noted to be a modified normal density for G_B with mean $\hat{\mu}_n$ and variance $(w_n p)^{-1}$. The parameter w_n , which will be referred to as the pseudovariance, was observed to be a measure of confidence in $\hat{\mu}_n$ as the true mean. Actually, the variance of G_B conditioned by the data is given by

$$\sigma^2 = \frac{r_n s_n}{(r_n - 3)w_n}.$$

The parameters r_n and s_n are defined in Equations 6.3.10 and 6.3.11 respectively. Since these parameters have little intuitive appeal, and since w_n is directly associated with $\hat{\sigma}_n^2$ as given by Equation 9.3.1, w_n will be taken as the measure of goodness of the estimation procedure, rather than the actual variance, for purposes of comparison to the empirical method.

The curves of Figure 9.3.1 afford a comparison of the empirical method to the unknown variance method, with the a priori values w_0^{-1} and $\hat{\mu}_0$ of one and zero degrees per hour respectively, for a sampling period of one second. For noise variance values greater than unity, the variance of the empirical estimate is always greater than the pseudovariance. The empirical variance is initially less than the pseudovariance for $\sigma_v^2 = 0.5$ but the situation reverses after about 40 seconds. In the time region illustrated, the pseudovariance is greater for $\sigma_v^2 = 0.1$.

This tendency was verified by the computer simulation results. To serve as a typical example, the results of an actual computer run are presented in Figure 9.3.2. The simulation conditions are as follows:

$$\begin{aligned} T &= 1.0 \text{ sec} \\ G_B &= 1.0 \text{ degree/hr} \\ w_n^{-1} &= 0.1 \text{ degree}^2/\text{hr}^2 \\ \hat{\mu}_0 &= 0.0 \text{ degree/hr} \\ \sigma_v^2 &= 0.1 \text{ feet}^2/\text{sec}^2 \end{aligned}$$

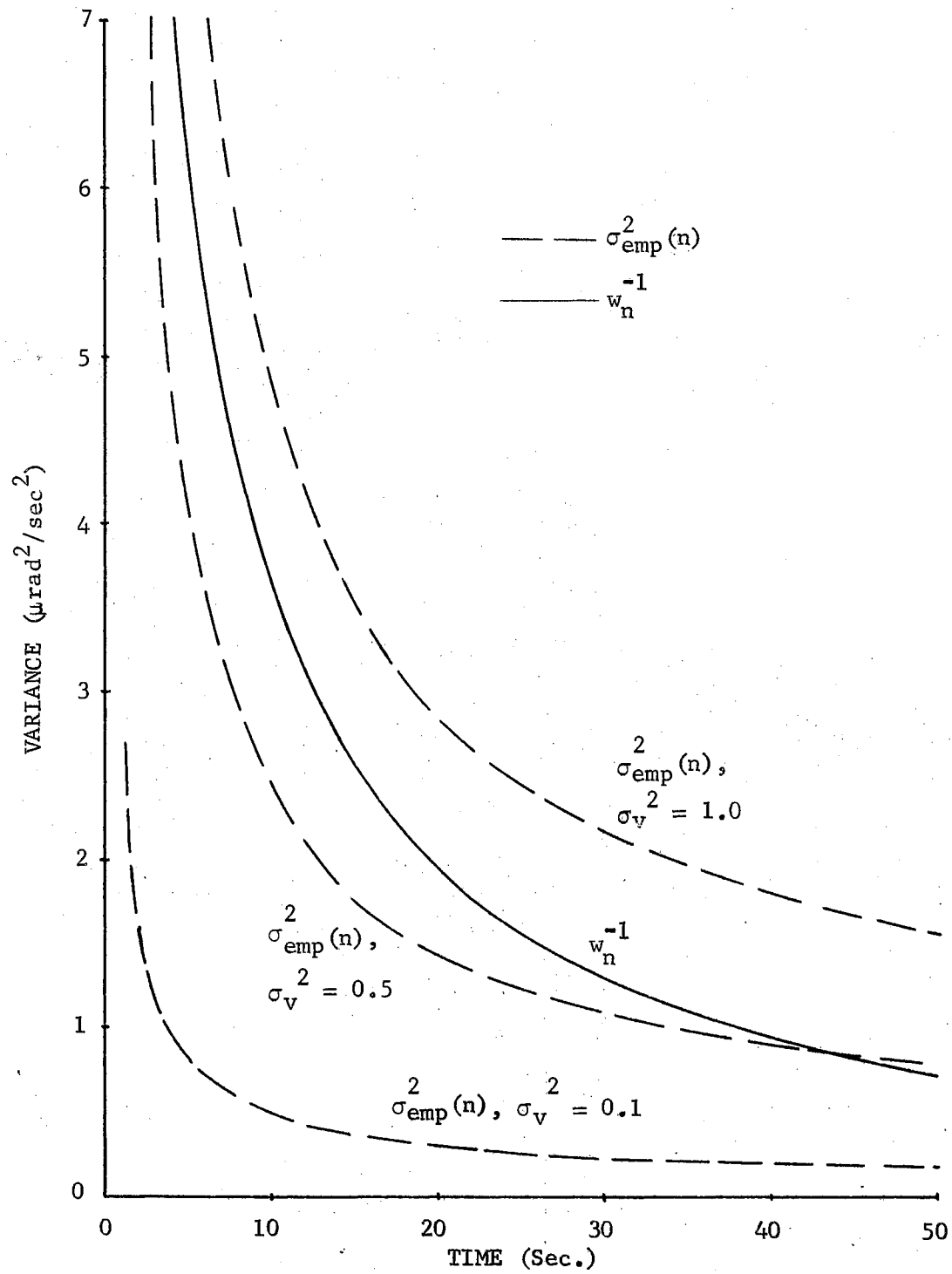


Figure 9.3.1. Empirical Variance and Pseudovariance

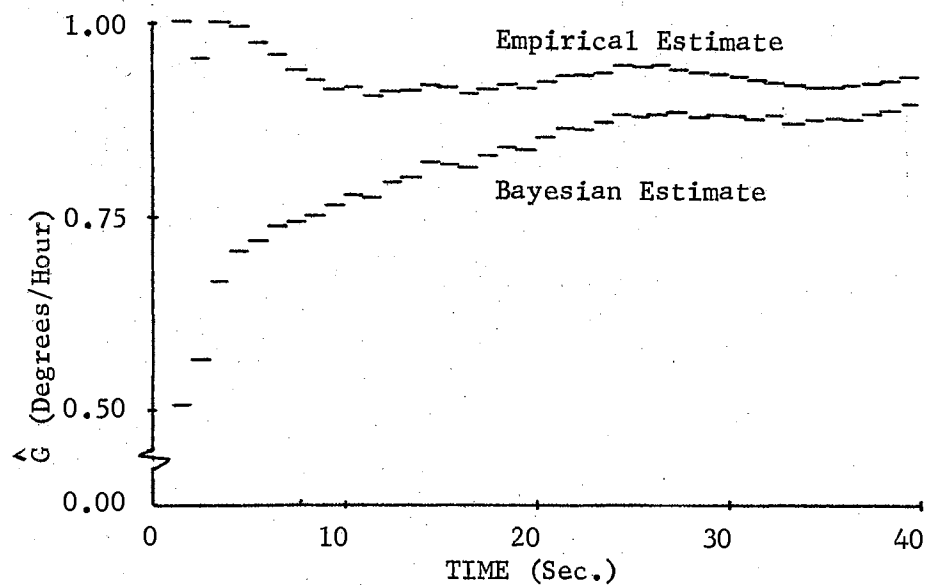


Figure 9.3.2. Simulation Results

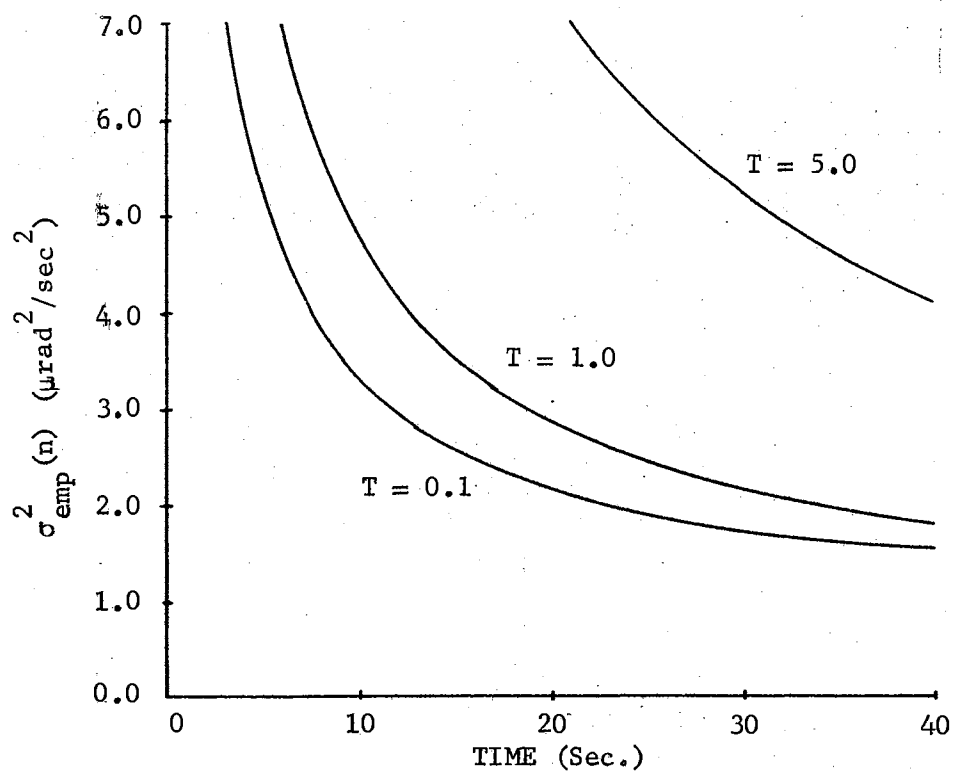


Figure 9.3.3. Effect of Sampling Period on Empirical Variance

Examination of the simulation results confirms the prediction that the empirical estimate is better for the stated conditions.

Thus one will note that there are conditions for which the empirical method has smaller errors than the Bayesian technique. Although the pseudovariance can be varied by changing the a priori parameter w_0 , there will still be values for the noise variance which result in better estimates from the empirical formulation.

The less confidence one has that the assumed density laws represent a true description of the random processes, the more he should be inclined to favor the empirical approach with its fewer assumptions. Moreover, if he uses the empirical formulation, he will be relieved of making a choice of the a priori parameters. Insofar as the empirical estimation requires no a priori knowledge, it may intuitively be considered self-adjusting to the actual noise conditions which is more in keeping with adaptive control system philosophy.

Figure 9.3.3 illustrates how changing the sampling period effects the squared error of the empirical estimate. The curves are for a σ_v of unity. One may again observe that the empirical method, for the sampling periods illustrated, is much faster than the third-order leveling method.

CHAPTER X

SUMMARY AND CONCLUSIONS

10.1 Summary. The system model was developed in Chapters II and III and the solution to the state equations was found.

Chapters IV through VII are devoted to development of the Bayesian learning algorithms under the assumption that the reference velocity error process is normal with variance σ_v^2 . For the case of σ_v known, the a priori density function of the gyro drift was assumed to be normal which is consistent with published experimental results. For σ_v unknown, p , the reciprocal of the variance σ_v^{-2} , was assumed to be a random variable and the joint a priori density function of p and the gyro drift was assumed to follow the Gaussian-inverted Wishart law (a modified Gaussian distribution).

In formulating the Bayesian solutions, the author chose to represent recursive estimates and covariance matrices similar to a Kalman formulation. This was done only after he had repeated failures with more direct approaches which tended to mask statistical dependence of the noise drivers and the observations. The uninitiated reader, working similar problems, might avoid this pitfall by using the Kalman forms as a framework for the Bayesian learning procedure.

The empirical estimation procedure was developed in Chapter VIII. Recursive forms of the estimate and the expected squared error were established.

The characteristics of the various estimation techniques were presented in Chapter IX. Also some comparisons were made with emphasis on the expected squared error.

10.2 Conclusions. For sampling periods less than twenty seconds, the empirical method and the Bayesian methods converged to the true value of gyro drift much faster than the conventional third-order leveling method. With the assumption that the velocity variance was specified, the Bayesian learning technique resulted in the minimum mean squared error of the estimate.

When this assumption was relaxed, the Bayesian learning procedure was still found to give a satisfactory estimate of the gyro drift. However, for low values of unknown reference velocity noise, the empirical estimation method was found to result in smaller mean squared error values than the Bayesian technique; for large noise variances, the opposite situation existed.

A recursive form of the estimate was found for the empirical method which is very desirable for digital computer mechanization. The empirical formulation has the distinct practical advantage of requiring a minimum knowledge of the velocity error random process and of the gyro drift. In this sense, it better represents an adaptive-learning philosophy.

10.3 Recommendations for Further Study. An interesting extension of this thesis would be to consider the problem of finding an optimum sampling period in a decision theoretic framework. It would be necessary to select some cost function, or criteria of goodness, and to assume a more complete system model. One could consider, for

example, the trade off between performance and equipment complexity.

In considering the problem of finding the Bayesian estimate, when the noise variance was unknown, the problem was formulated using the Gaussian-inverted Wishart joint a priori density function. Essentially the gyro drift and the noise variance were learned. The gyro drift estimate was used in a feedback loop to cancel the gyro drift. The estimate of the noise variance was not formed explicitly since it was not needed to satisfy the stated optimality criteria. The learned variance could perhaps be used to satisfy a different criteria such as finding the minimum mean square estimate of actual system velocity.

BIBLIOGRAPHY

1. Abramson, N. and D. Braverman. "Learning to Recognize Patterns in a Random Environment." IRE Transactions on Information Theory. Vol. IT-8. (September, 1962).
2. Aoki, Masanao. Optimization of Stochastic Systems. New York: Academic Press Inc., 1967.
3. Breipohl, A. M. and A. H. Koschmann. "Adaptive Communication Systems." Technical Report EE-98, University of New Mexico, Engineering Experiment Station, (August, 1963).
4. Dushman, Allan. "On Gyro Drift Models and Their Evaluation." IRE Transactions on Aerospace and Navigational Electronics. Vol. ANE-9. (December, 1962).
5. Hammon, Robert L. "Effects on Inertial Guidance Systems of Random Error Sources." IRE Transactions on Aerospace and Navigational Electronics. Vol. ANE-9. (December, 1962).
6. Ho, Y. C. and R. C. K. Lee. "A Bayesian Approach to Problems in Stochastic Estimation and Control." IEEE Transactions on Automatic Control. Vol. AC-9. (October, 1964).
7. Kalman, R. E. "A New Approach to Linear Filtering and Prediction Problems." Transactions of the ASME. Vol. 82. (March, 1960).
8. Keehn, D. G. "Learning the Mean Vector and Covariance Matrix of Gaussian Signals in Pattern Recognition." TR NO 2003-6. Stanford, California: Stanford Electronics Laboratories, Stanford University, 1963.
9. Koenig, Herman E., Yilmaz Tokad, and Hiremaglur K. Kesevan. Analysis of Discrete Physical Systems. New York: McGraw-Hill, 1967.
10. McClure, Connie L. Theory of Inertial Guidance. Englewood Cliffs: Prentice-Hall, Inc., 1960.
11. Miller, Kenneth S. Multidimensional Gaussian Distributions. New York: J. Wiley and Sons, 1964.
12. Nilsson, Nils J. Learning Machines. New York: McGraw-Hill, 1965.

13. Papoulis, Athanasios. Probability, Random Variables, and Stochastic Processes. New York: McGraw-Hill, 1965.
14. Parvin, Richard H. Inertial Navigation. Princeton: D. Van Nostrand Company, Inc., 1962.
15. Weiss, Lionel. Statistical Decision Theory. New York: McGraw-Hill, 1961.

APPENDIX A

EVALUATING THE TRANSITION MATRIX

Of many methods which are available to find the transition matrix $\underline{e}^{\underline{A}t}$, the particular method used here, which is called the constituent matrix method (9), is to expand $[\underline{sU} - \underline{A}]^{-1}$ in partial fractions about the eigenvalues. Thus the form will be

$$\underline{e}^{\underline{A}t} = \underline{C}_1 e^{l_1 t} + \underline{C}_2 e^{l_2 t} + \underline{C}_3 e^{l_3 t}$$

where the \underline{C}_i matrix is called the constituent matrix associated with the i^{th} eigenvalue.

By direct substitution, one can obtain

$$[\underline{sU} - \underline{A}] = \begin{bmatrix} s & g & K_1 \\ -1/R & s & K_2/R \\ -b & g & s+K_1+b \end{bmatrix} \quad (\text{A.1})$$

and its inverse

$$[\underline{sU} - \underline{A}]^{-1} = \begin{bmatrix} s^2 + s(K_1+b) + \frac{g}{R} K_2 & -g(s+b) & -K_1 s + \frac{gK_2}{RK_1} \\ s+K_1+b(1+K_2) & (s+K_1)(s+b) & \frac{K_2}{R}s - \frac{K_1}{K_2} \\ bs - \frac{g}{R} & -g(s+b) & s^2 + \frac{g}{R} \end{bmatrix} \quad (\text{A.2})$$

$$(s+b)[(s+a)^2 + w^2]$$

where $a = K_1/2$ and $w = [g(1 + K_2/R - a^2)]^{1/2}$. The reader will recall that $b = 1$. Using the formula

$$\underline{C}_1 = (s + 1_i)[s\underline{U} - \underline{A}]^{-1} \Big|_{s = -1_i}, \quad (\text{A.3})$$

one can obtain the following constituent matrices:

For $s = -b = -1$,

$$\underline{C}_1 = \frac{\begin{bmatrix} -K_1 + gK_2/R & 0 & K_1 + gK_2/R \\ (K_1 + K_2)/R & 0 & -(K_1 + K_2)/R \\ -(1 + g/R) & 0 & 1 + g/R \end{bmatrix}}{1 - K_1 + g(1 + K_2)/R} \quad (\text{A.4})$$

For $s = -a + jw$,

$$\underline{C}_2 = \frac{\begin{bmatrix} jw - a - \frac{g}{R} & -g(jw - a + 1) & -2jaw + 2a^2 - \frac{gK_2}{R} \\ \frac{jw + a + (1+K_2)}{R} & jw + a - \frac{g}{R}(1+K_2) & jwK_2 - K_1(1+K_2) \\ jw - a - \frac{g}{R} & -g(jw - a + 1) & -2jaw + 2a^2 - \frac{gK_2}{R} \end{bmatrix}}{(j2w)(1 + jw - a)}, \quad (\text{A.5})$$

and finally one will note that, for $s = -jw - a$,

$$\underline{C}_3 = \text{conj}(\underline{C}_2) \quad (\text{A.6})$$

where $\text{conj}(\cdot)$ is the complex conjugate.

Expressing the complex exponential terms as sines and cosines, collecting the real and imaginary parts of \underline{C}_2 and \underline{C}_3 and substituting the numerical values results in the following expression for the transition matrix:

$$e^{\frac{A}{\omega}t} = \begin{bmatrix} .02025 & 0.0 & .02025 \\ 4.883 \times 10^{-6} & 0.0 & -4.883 \times 10^{-6} \\ -1.020 & 0.0 & 1.020 \end{bmatrix} e^{-t} + \quad (A.7)$$

$$\begin{bmatrix} 1.020 & 0.0 & -.02025 \\ -4.883 \times 10^{-6} & 1.0 & 4.883 \times 10^{-6} \\ 1.020 & 0.0 & -.02025 \end{bmatrix} e^{-.01t} \cos(.00746t)$$

$$\begin{bmatrix} 1.346 & 4316. & -.006067 \\ -6.543 \times 10^{-4} & -1.346 & -6.571 \times 10^{-6} \\ 1.346 & 4316. & -.006067 \end{bmatrix} e^{-.01t} \sin(.00746t)$$

Only the second column of the transition matrix has appearance simple enough to warrant expression in terms of the literal system parameters. This column can be obtained by taking the inverse Laplace transform of the second column of Equation A.2 as follows:

$$\text{col}_2 = \mathcal{L}^{-1} \frac{\begin{bmatrix} -g \\ s + 2a \\ -g \end{bmatrix}}{(s + a)^2 + w^2}$$

$$= \begin{bmatrix} - (ge^{-at} \sin wt)/w \\ e^{-at} (\cos wt + \frac{a}{w} \sin wt) \\ - (ge^{-at} \sin wt)/w \end{bmatrix} \quad (A.8)$$

The following integrals of Equation A.8 are used in the body of

this thesis:

$$\underline{\theta} = \int_0^T \text{col}_2 \, dt \quad (\text{A.9})$$

$$\hat{\underline{\theta}}_0 = \int_0^\infty \text{col}_2 \, dt. \quad (\text{A.10})$$

By direct integration, these integrals are found to be

$$\underline{\theta} = \frac{R}{1 + K_2} \begin{bmatrix} -(1 - e^{-aT} \cos wT) + (ae^{-aT} \sin wT)/w \\ \frac{2a(1 - e^{-aT} \cos wT)}{g} + \frac{(w^2 - a^2)e^{-aT} \sin wT}{wg} \\ -(1 - e^{-aT} \cos wT) + (ae^{-aT} \sin wT)/w \end{bmatrix} \quad (\text{A.11})$$

$$\hat{\underline{\theta}}_0 = \frac{R}{1 + K_2} \begin{bmatrix} -1 \\ K_1/G \\ -1 \end{bmatrix}. \quad (\text{A.12})$$

APPENDIX B

CONDITIONAL EXPECTED VALUES AND RELATIONSHIPS

B.1 Introduction. Several properties of the various expected values will be established in this appendix. The case for σ_v known is first treated and then the case for σ_v unknown is shown to be similar with a slight modification.

B.2 Expected Value of \underline{g}_n . The reader will recall the following definitions for \underline{g}_n :

$$\underline{g}_0 = \sigma_v \sqrt{2b} \int_{-\infty}^0 \underline{\phi}(-x) \underline{B}_2 v(x) dx \quad (\text{B.2.1})$$

$$\underline{g}_n = \sigma_v \sqrt{2b} \int_{nT-T}^{nT} \underline{\phi}(nT - x) \underline{B}_2 v(x) dx, \quad n \geq 1 \quad (\text{B.2.2})$$

where

$$\underline{B}_2 = \begin{bmatrix} 0 \\ 0 \\ 1 \end{bmatrix} \quad (\text{B.2.3})$$

$$E[v(x)] \equiv 0 \quad (\text{B.2.4})$$

$$E[v(x)v(y)] = \delta(x - y). \quad (\text{B.2.5})$$

The vector \underline{g}_n can be displayed in terms of the elements of the transition matrix through the use of Equation B.2.3 and the notation $\underline{\phi}(t) = [\phi_{ij}(t)]$ to obtain

$$\underline{g}_n = \sigma_v \sqrt{2b} \int_{nT-T}^{nT} \begin{bmatrix} \phi_{13}(nT - t) \\ \phi_{23}(nT - t) \\ \phi_{33}(nT - t) \end{bmatrix} v(t) dt, \quad n \geq 1. \quad (\text{B.2.6})$$

Using Equations B.2.1 and B.2.4 with an interchange of expected value and integration, one can perform the following steps:

$$\begin{aligned} E(\underline{g}_0) &= E[\sigma_v \sqrt{2b} \int_{-\infty}^0 \underline{\phi}(-x) \underline{B}_2 v(x) dx] \\ &= \sigma_v \sqrt{2b} \int_{-\infty}^0 \underline{\phi}(-x) \underline{B}_2 E[v(x)] dx \\ &= 0. \end{aligned} \quad (\text{B.2.7})$$

Similarly, one can show $E(\underline{g}_n) = 0$ for $n \geq 1$ and obtain

$$E(\underline{g}_n) = 0, \quad n \geq 0. \quad (\text{B.2.8})$$

B.3 Variance of \underline{g}_n . In a like manner, using Equations B.2.1 and B.2.5 along with an interchange of expectation and integration, one may proceed

$$\begin{aligned} E(\underline{g}_0 \underline{g}_0^T) &= E[2b\sigma_v^2 \int_{-\infty}^0 \underline{\phi}(-x) \underline{B}_2 v(x) dx \int_{-\infty}^0 \underline{B}_2^T \underline{\phi}^T(-y) v(y) dy] \\ &= 2b\sigma_v^2 \int_{-\infty}^0 \underline{\phi}(-x) \underline{B}_2 \underline{B}_2^T \underline{\phi}^T(-x) dx. \end{aligned} \quad (\text{B.3.1})$$

Similarly, for $n \geq 1$,

$$E(\underline{g}_n \underline{g}_n^T) = 2b\sigma_v^2 \int_{nT-T}^{nT} \underline{\phi}(nT - x) \underline{B}_2 \underline{B}_2^T \underline{\phi}^T(nT - x) dx \quad (\text{B.3.2})$$

but this equation can be further reduced by a single change of variable of integration to

$$E(\underline{g}_n \underline{g}_n^T) = 2b\sigma_v^2 \int_0^T \underline{\phi}(T-t) \underline{B}_2 \underline{B}_2^T \underline{\phi}^T(T-t) dt, \quad n \geq 1 \quad (\text{B.3.3})$$

or

$$E(\underline{g}_n \underline{g}_n^T) = E(\underline{g}_1 \underline{g}_1^T), \quad n \geq 1. \quad (\text{B.3.4})$$

The covariance matrix $E(\underline{g}_1 \underline{g}_1^T)$ will be denoted as \underline{H} ; hence

$$E(\underline{g}_n \underline{g}_n^T) = \underline{H}, \quad n \geq 1. \quad (\text{B.3.5})$$

If $m \geq 1$ and $n \geq 1$ with $m \neq n$, then

$$E(\underline{g}_m \underline{g}_n^T) = 2b\sigma_v^2 \int_{mT-T}^{mT} \int_{nT-T}^{nT} \underline{\phi}(mT-x) \underline{B}_2 \underline{B}_2^T \underline{\phi}^T(nT-y). \quad (\text{B.3.6})$$

$$E[v(x)v(y)] dy dx$$

but, since the variables x and y are in non-overlapping intervals, it follows from Equation B.2.5 that

$$E(\underline{g}_m \underline{g}_n^T) = \underline{0}, \quad m \neq n. \quad (\text{B.3.7})$$

The restriction that $m \geq 1$ and $n \geq 1$ is omitted in Equation B.3.7 since an identical argument would be valid if $m = 0$, $n \neq 0$ or $m \neq 0$, $n = 0$.

B.4 Recursive Properties of Conditional Expectations. In Chapter VII it is shown that \hat{G}_n is a linear combination of the variables $y(nT)$ which followed from a property of normal distributions. This result is used in this section.

Property B.4.1. For $n > 0$, $\underline{z}(nT)$ is a linear combination of the $n+2$ random variables $\underline{G}_B, \underline{g}_0, \dots, \underline{g}_n$.

Proof:

The notation $L_n(G_B, \underline{g}_0, \dots, \underline{g}_n)$ will be used to symbolize a linear combination of the variables; the proof will be by induction.

$$1. \text{ Now } \underline{z}(0) = \underline{g}_0 + \underline{g}_B; \text{ hence } \underline{z}(0) = L_0(G_B, \underline{g}_0).$$

$$\begin{aligned} 2. \text{ Also } \underline{z}(T) &= \underline{\phi}(T)\underline{z}(0) + (G_B - \hat{G}_0)\underline{\theta} + \underline{g}_1 \\ &= \underline{\phi}(T)L_0(G_B, \underline{g}_0) + (G_B - \hat{G}_0)\underline{\theta} + \underline{g}_1 \\ &= L_1(G_B, \underline{g}_0, \underline{g}_1) \end{aligned}$$

since \hat{G}_0 is a linear combination of $\hat{\mu}_0$ and \underline{g}_0 .

$$3. (a) \text{ Assume } \underline{z}(nT) = L_n(G_B, \underline{g}_0, \dots, \underline{g}_n).$$

$$(b) \text{ Recall } \underline{z}(nT + T) = \underline{\phi}(T)\underline{z}(nT) + (G_B - \hat{G}_n)\underline{\theta} + \underline{g}_{n+1};$$

$$\begin{aligned} \text{hence } \underline{z}(nT + T) &= \underline{\phi}(T)L_n(G_B, \underline{g}_0, \dots, \underline{g}_n) + \\ &\quad (G_B - \hat{G}_n)\underline{\theta} + \underline{g}_{n+1}. \end{aligned}$$

(c) But since \hat{G}_n is a linear combination of $\hat{\mu}_0$ and $\underline{y}(nT)$,
and $\underline{y}(nT) = \underline{C} \underline{z}(nT)$, then

$$\underline{z}(nT + T) = L_{n+1}(G_B, \underline{g}_0, \dots, \underline{g}_n, \underline{g}_{n+1}),$$

and the theorem follows.

Since G_B and $v(t)$ are independent and normal, \underline{g}_n is a normal random variable which is statistically independent of G_B . Moreover, from Equations B.2.8 and B.3.7, it follows that \underline{g}_n and \underline{g}_m are independent if $n \neq m$; therefore, the $n+2$ random variables $G_B, \underline{g}_0, \dots, \underline{g}_n$ are jointly-normal, statistically independent random variables. From this

fact and Property B.4.1, and from Equations B.2.8, B.3.5, and B.3.7, one reaches the immediate conclusions:

Property B.4.2. $E[\underline{g}_n | G_B] = 0, n = 0, 1$

$$E[\underline{g}_n | G_B, \underline{y}(nT - T)] = 0, n \geq 2.$$

Property B.4.3. $E[\underline{g}_m \underline{g}_n | G_B, \underline{y}(nT - T)] = 0, m \neq n, m \geq 0, n \geq 1.$

Property B.4.4. $E[\underline{g}_n \underline{g}_n^T | G_B, \underline{y}(nT - T)] = \underline{H}, n \geq 1.$

The following two properties establish transitional relationships of the estimates.

Property B.4.5. For $n \geq 1$, $\hat{\underline{z}}'_n = \underline{\varnothing}(T) \hat{\underline{z}}_{n-1} + (G_B - \hat{G}_{n-1}) \underline{\vartheta}.$

Proof:

1. From Equations 4.2.4, 5.4.6, and 5.4.7,

$$\begin{aligned} \hat{\underline{z}}'_n &= E[\underline{z}(nT) | G_B, \underline{y}(nT - T)] \\ &= E\left\{ \left[\underline{\varnothing}(T) \underline{z}(nT - T) + (G_B - \hat{G}_{n-1}) \underline{\vartheta} + \underline{g}_n \right] \middle| \right. \\ &\quad \left. G_B, \underline{y}(nT - T) \right\}. \end{aligned}$$

2. Using the linearity property of the conditional expectation along with Equations 5.4.1 and 5.4.2, and Property B.4.2, one can write

$$\hat{\underline{z}}'_n = \underline{\varnothing}(T) \hat{\underline{z}}_{n-1} + \underline{\vartheta} E[(G_B - \hat{G}_{n-1}) | G_B, \underline{y}(nT - T)]$$

or

$$\hat{\underline{z}}'_n = \underline{\emptyset}(T) \hat{\underline{z}}_{n-1} + (G_B - \hat{G}_{n-1}) \underline{\emptyset},$$

which was to be established.

Property B.4.6. For $n \geq 1$, $\underline{P}_n^* = \underline{\emptyset}(T) \underline{P}_{n-1} \underline{\emptyset}^T(T) + \underline{H}$.

Proof:

1. From Equations 4.2.4, 5.4.3, and 5.4.8, and Property B.4.5 above, one can perform the following steps:

$$\begin{aligned} \underline{e}'_n &= \underline{z}(nT) - \hat{\underline{z}}'_n \\ &= \underline{\emptyset}(T) \underline{z}(nT - T) + (G_B - \hat{G}_{n-1}) \underline{\emptyset} + \underline{g}_n \\ &\quad - \underline{\emptyset}(T) \hat{\underline{z}}_{n-1} + (G_B - \hat{G}_{n-1}) \underline{\emptyset} \\ &= \underline{\emptyset}(T) \underline{e}_{n-1} + \underline{g}_n. \end{aligned}$$

2. Using the result of step 1, along with Equations 5.4.9 and 5.4.10, one can continue

$$\begin{aligned} \underline{P}_n^* &= E[\underline{e}'_n \underline{e}'_n{}^T | G_B, \underline{y}(nT - T)] \\ &= E[\underline{\emptyset}(T) \underline{e}_{n-1} \underline{e}_{n-1}{}^T \underline{\emptyset}^T(T) + \underline{\emptyset}(T) \underline{e}_{n-1} \underline{g}_n{}^T + \underline{g}_n \underline{e}_{n-1}{}^T \underline{\emptyset}^T(T) \\ &\quad + \underline{g}_n \underline{g}_n{}^T | G_B, \underline{y}(nT - T)] \\ &= E[\underline{\emptyset}^T(T) \underline{e}_{n-1} \underline{e}_{n-1}{}^T \underline{\emptyset}(T) + \underline{g}_n \underline{g}_n{}^T | G_B, \underline{y}(nT - T)] \end{aligned}$$

where the last step is valid since \underline{g}_n is independent of the other variables and \underline{g}_n has zero mean.

3. Making use of Equations 5.4.4 and 5.4.5, and Property B.4.4, one finally obtains the desired result

$$\underline{P}_n^* = \underline{\phi}(T) \underline{P}_{n-1} \underline{\phi}^T(T) + \underline{H}.$$

B.5 Modifications for the Case of Unknown σ_v . The previous work in this appendix rests on the assumption that σ_v is known (taken numerically as unity). Since this assumption is relaxed elsewhere in this thesis, some modifications must be made in the preceding equations.

When σ_v is not known, σ_v^2 is set equal to $1/p$ and thereafter treated as a random variable (analogous to G_B). Thus all of the above conditional expectations will also have p as an additional condition, for example $E[\underline{z}(T) | p, G_B, y(T)]$, and the equations involving \underline{g}_n will have p^{-1} appearing in place of σ_v^2 ; for example,

$$\underline{g}_0 = (2b/p)^{1/2} \int_{-\infty}^0 \underline{\phi}(-x) \underline{B}_2 v(x) dx.$$

To minimize the impact on notation, the symbolization for the various means and conditional estimates will not be changed and only a slight change will be made in the equations involving covariance terms; specifically a factor of p^{-1} will appear. The symbols $\hat{\underline{z}}_n$, \underline{P}_n^* , etc., will be used for both cases of σ_v known and unknown since no confusion will result because they are always treated in separate sections.

It is shown in Chapter VII that the optimum estimate \hat{G}_n of G_B given the measurement remains a linear combination of $\hat{\mu}_0$ and $\underline{y}(nT)$. Moreover, the following equations are valid as can be shown by a trivial change in previous arguments:

$$E(\underline{g}_n | p, G_B) = 0, \quad n = 0, 1.$$

$$E[\underline{g}_n | p, G_B, \underline{y}(nT - T)] = 0, \quad n \geq 2.$$

Since $\sigma_V = 1.0$,

$$\begin{aligned} E(\underline{g}_1 \underline{g}_1^T | p) &= (2b/p) \int_0^T \underline{\varnothing}(T-x) \underline{B}_2 \underline{B}_2^T \underline{\varnothing}^T(T-x) dx \\ &= \underline{H}/p . \end{aligned}$$

Also, one can write

$$E[\underline{g}_n \underline{g}_n^T | p, G_B, \underline{y}(nT - T)] = \underline{H}/p, \quad n \geq 2$$

$$E[\underline{g}_n \underline{g}_1^T | p, G_B] = \underline{0}, \quad n \geq 2, \quad n = 0$$

$$E[\underline{g}_m \underline{g}_n^T | p, G_B, \underline{y}(nT - T)] = \underline{0}, \quad n \geq 2, \quad m \neq n.$$

A more complete discussion of the changes is presented in Section

5.4.

APPENDIX C

CONVERGENCE AND STABILITY

C.1 Introduction. In this appendix convergence of the Bayesian a posteriori density function to the actual gyro drift value is considered for the case of known σ_v . To simplify the discussion, it will be assumed that the learning loop is open; that is, the estimate of G_B is computed but it is not applied as a control signal. The results can readily be extended to the closed loop case, i.e., using the estimate as a control signal, by observing that the closed loop formulation merely accounts for the fact that there is a control signal.

Convergence for Bayesian learning for the case of unknown σ_v is not specifically discussed in this appendix because it can be established by a nearly identical argument.

Since stability is often a problem in closed loop control systems, a brief discussion of stability is also presented in the final section of this appendix.

C.2 Convergence of the Bayesian Estimate. The inertial system is operated with some unknown value G_B of constant gyro drift and a sequence of measurements is observed from which an estimate of the gyro drift value is to be constructed. Over the operating period, this value remains constant. If the system is shut off, allowed to cool, and started again, the gyro drift will assume some new value for the second period of operation.

Consistent with the Bayesian approach (13), G_B is assumed to be a random variable. The probability density function of G_B is assumed to be normal with mean $\hat{\mu}_0$ and positive variance $\hat{\sigma}_0^2$.

Each measurement $y(kT)$ is a random variable which is a known function of the gyro drift and of a convolution of the random reference velocity error process; this functional relationship is dictated by the assumed state model. Estimates of G_B , which were constructed as linear combinations of the measurements, are also random variables.

It is important in the following discussion to distinguish between the random variables $\underline{y}(kT)$ and actual data y_k . In this appendix, the random variable $\underline{y}(kT)$ will be referred to as measurements and \underline{y}_n , which is a set of measured values or a sample function, will be referred to as data.

The estimates of G_B , empirical as well as Bayesian, have been observed to be random variables which are functions of the measurements. The equations developed for these estimates specify how one is to construct numerical estimates from the data. Here again, one needs to distinguish a random variable, the estimate, from a number, the estimate of G_B given the data.

In Chapter VIII, the empirical estimate, which will be denoted as \hat{G}_e in this appendix to distinguish it from the Bayesian estimates \hat{G}_n , was formed as

$$\hat{G}_e(n) = \frac{1}{\theta_{03}} \sum_{k=1}^n \frac{y(kT)}{n}, \quad n \geq 1 \quad (C.2.1)$$

and the mean square error

$$\sigma_{\text{emp}}^2(n) = E\left\{[\hat{G}_e(n) - G_B]^2\right\}, \quad n \geq 1 \quad (C.2.2)$$

was found to approach zero as n became infinite

$$\lim_{n \rightarrow \infty} \sigma_{\text{emp}}^2(n) = 0. \quad (\text{C.2.3})$$

The empirical estimate is formed without any knowledge of the probability density functions of either G_B or the noise driver. If, in fact, the random variable G_B is known to be normal with mean $\hat{\mu}_0$ and variance $\hat{\sigma}_0^2$ and the reference velocity error is known to be normal with variance σ_v^2 , the empirical estimate is constructed exactly as though this information is not known. In other words, the empirical estimate ignores, or is independent of, the a priori knowledge.

The optimal Bayesian estimate, with σ_v known, is given by

$$\hat{G}_n = E[G_B | \underline{y}(nT)], \quad n \geq 1. \quad (\text{C.2.4})$$

Presented data \underline{y}_n , the numerical Bayesian estimate is evaluated as

$$\hat{\mu}_n = \hat{G}_n \Big|_{\underline{y}(nT) = \underline{y}_n}, \quad n \geq 1. \quad (\text{C.2.5})$$

The mean square error of the estimate \hat{G}_n is

$$E[(\hat{G}_n - G_B)^2] = E\{E[(\hat{G}_n - G_B)^2 | \underline{y}(nT)]\}, \quad n \geq 1 \quad (\text{C.2.6})$$

which becomes, for the numerical estimate $\hat{\mu}_n$ given the data \underline{y}_n ,

$$\hat{\sigma}_n^2 = E[(\hat{\mu}_n - G_B)^2 | \underline{y}(nT) = \underline{y}_n], \quad n \geq 1. \quad (\text{C.2.7})$$

In the following theorem, it is shown that this error becomes arbitrarily small as more data is obtained.

Theorem C.2.1. Given a sequence of data \underline{y}_n , the mean squared error $\hat{\sigma}_n^2$, as expressed by Equation C.2.7, of the numerical Bayesian esti-

mate $\hat{\mu}_n$ of Equation C.2.5 tends to zero as the sample size increases without bound; that is,

$$\lim_{n \rightarrow \infty} \hat{\sigma}_n^2 = 0. \quad (\text{C.2.8})$$

Proof:

The Bayesian estimate of Equation C.2.4 is known (13) to be a function of the measurements which results in the minimum expected squared error as given by Equation C.2.6. Given data, the Bayesian numerical is computed from Equation C.2.4 and the associated mean squared error is expressed by Equation C.2.7.

The empirical estimate is, in general, a different function of the measurements and therefore its expected squared error can be no less than the minimum; it follows that

$$\hat{\sigma}_n^2 \leq \sigma_{\text{emp}}^2(n). \quad (\text{C.2.9})$$

Combining the properties expressed by Equations C.2.3 and C.2.9, the conclusion of Equation C.2.8 follows.

It is interesting to observe that Figure 9.2.5 illustrates the Inequality C.2.9.

C.3 Convergence of the Bayesian a posteriori Density Function.

Convergence, with probability one, of the numerical estimate to G_B is established by the following theorem.

Theorem C.3.1. Under the hypothesis of Theorem C.2.1,

$$|\hat{\mu}_n - G_B| \rightarrow 0, \text{ with probability one, as } n \rightarrow \infty.$$

Proof:

It is desired to show, that for every $\epsilon > 0$, $P(|\hat{\mu}_n - G_B| \geq \epsilon) \rightarrow 0$ as $n \rightarrow \infty$. From Tchebycheff's inequality,

$$P(|\hat{\mu}_n - G_B| \geq \epsilon) = 1 - 2 \operatorname{erf}(\epsilon/\hat{\sigma}_n).$$

Since, from Theorem C.2.1, $\lim_{n \rightarrow \infty} \hat{\sigma}_n = 0$ and the conclusion follows.

Intuitively, the results of the above two theorems imply that as the data sample gets larger, the a posteriori density function approaches an impulse or spike centered about G_B .

C.4 Stability with the Learning Loop. The question of stability is answered as a result of convergence of the estimate to the true gyro drift value. In the empirical case, n^{-1} appears as a factor or weight of the n^{th} measurement. Therefore, as n gets very large, the effective gain of the loop goes to zero and the system behavior approaches that of the original system before the learning loop was added. Or, from a different viewpoint, the difference between gyro drift and its estimate acts as a system driver and, since the difference converges to zero, the driver tends to zero.

For the Bayesian estimate, with known variance, a similar situation exists for σ_n^2 tends to zero as n approaches infinity. In the unknown variance case, w_n^{-1} also tends to zero. Therefore, convergence of the estimate to the true value implies stability.

APPENDIX D

THIRD-ORDER LEVELING

A well established method (10) to cancel the gyro bias is illustrated by the error model of Figure D.1. The value of the control constants K_1 , K_2 , and K_3 are often chosen to give a critically damped system with some specified time constant. It will be assumed that the system constants are as follows:

$$K_1 = 0.03$$

$$K_2 = 194$$

$$K_3 = 0.649.$$

The above selection of values will result in a critically damped system with a 100 second time constant or

$$a = 0.01.$$

It can be shown that the corrective signal $\hat{G}(t)$ has an expected time response given by

$$E[\hat{G}(t) | G_B] = -[1 - (1 + at + a^2 t^2/2) \exp(-at)] G_B \quad (D.1)$$

which is illustrated graphically in Figure D.2. The variance of $\hat{G}(t)$ is initially zero and grows to a steady-state value of about

$$\sigma_{\hat{G}}^2 = 2.7 \times 10^{-13} \text{ rad}^2/\text{sec}^2. \quad (D.2)$$

This compensation method, usually referred to as third-order leveling, is compared with the other methods in Chapter IX.

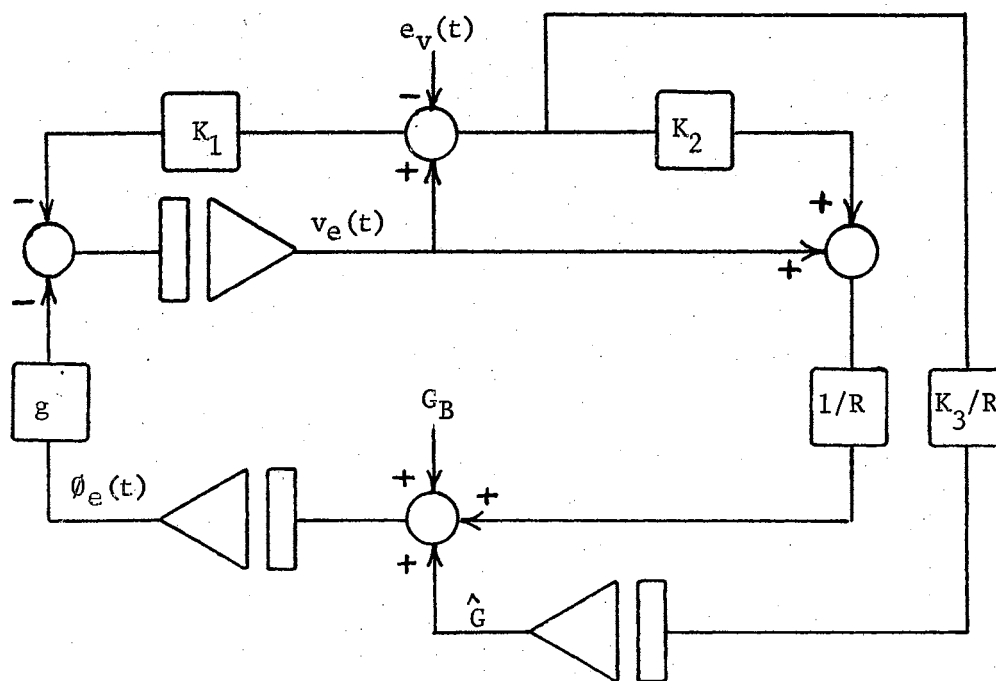


Figure D.1. Third-Order Leveling Loop

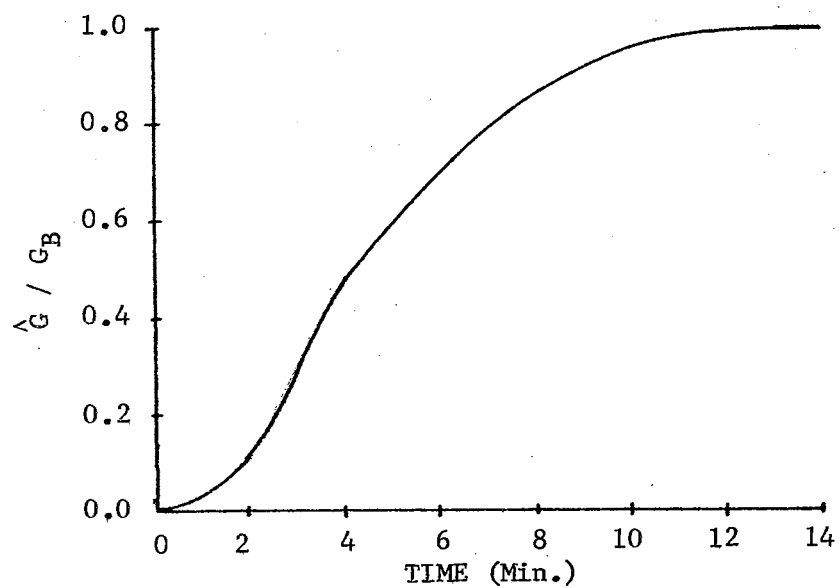


Figure D.2. Estimate Time Response

VITA

William Robert Barclay

Candidate for the Degree of

Doctor of Philosophy

Thesis: APPLICATION OF LEARNING TECHNIQUES TO AN INERTIAL NAVIGATION
SYSTEM

Major Field: Electrical Engineering

Biographical:

Personal Data: Born on December 20, 1936, in Duncan, Oklahoma,
the son of Ralph O. and Rachel H. Barclay.

Education: Attended primary and secondary schools in Duncan,
Oklahoma, and graduated from Duncan High School in May,
1955; attended the University of Oklahoma, Norman, Oklahoma;
received the Bachelor of Science degree in Electrical Engi-
neering from Oklahoma State University in May, 1960; re-
ceived the Master of Science degree in Electrical Engineering
from Wichita State University in August, 1963; completed
requirements for the Doctor of Philosophy degree in May,
1968.

Professional experience: Employed by Temco Aircraft, Dallas,
Texas, during the summer of 1960. Employed by The Boeing
Company, Wichita, Kansas, as a research engineer from
August, 1960, to September, 1964, and during the summer
of 1965. Employed by the School of Electrical Engineering
of Oklahoma State University as a graduate assistant from
September, 1964, to May, 1967.

Professional organizations: Member of the Institute of Electrical
and Electronic Engineers.